电子科技大学

University of Electronic Science and Technology of China

9 Nanoholes array and polarization effect

物理电子学院

School of Physical Electronics

巴比涅原理（Babinet principle）

<u>巴比涅原理</u>：在点光源照明下，两个互补的衍射屏 $u_0(x,y)$、$u_c(x,y)$在与点光源共轭的平面上，除了点光源的几何像点外，两者有着相同的**夫琅禾费衍射**图样。

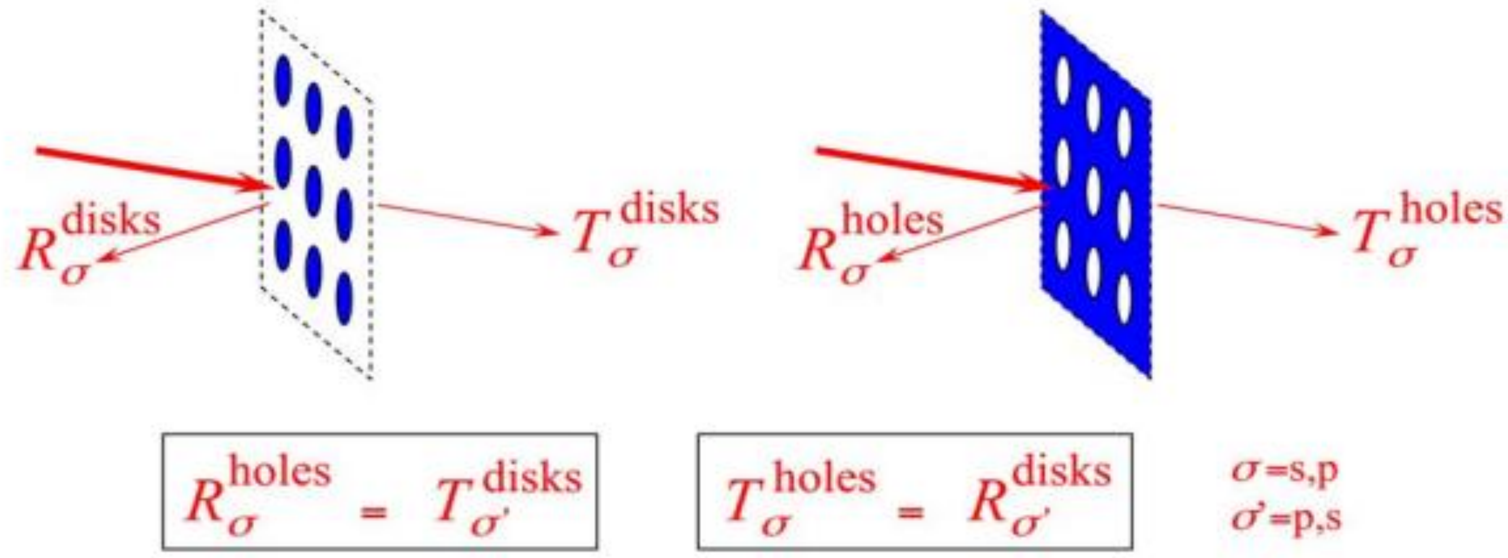

FIG. 5. (Color online) Babinet's principle applied to disk and hole arrays. The transmittance (reflectance) of the disk array for light of a given polarization σ (s or p) is identical to the reflectance (transmittance) of the complementary hole array for orthogonal polarization σ' (p or s, respectively).

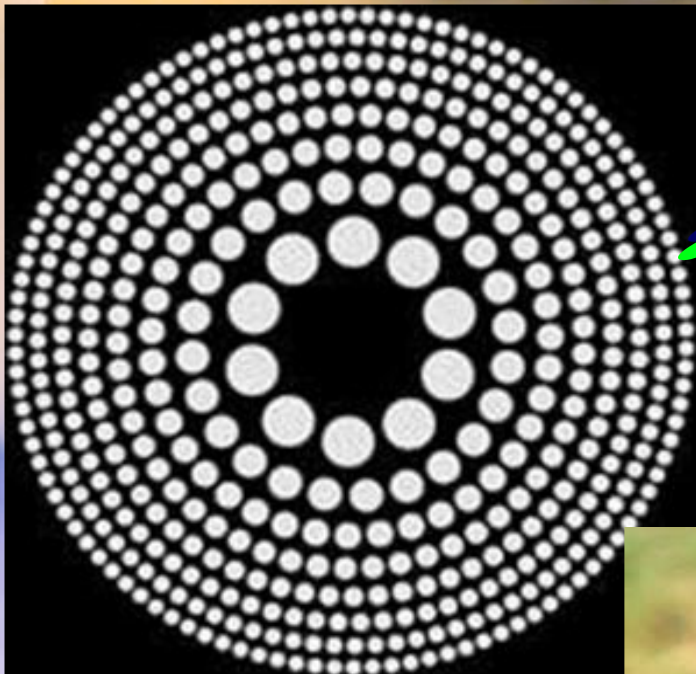

圆斑circular disk

? =

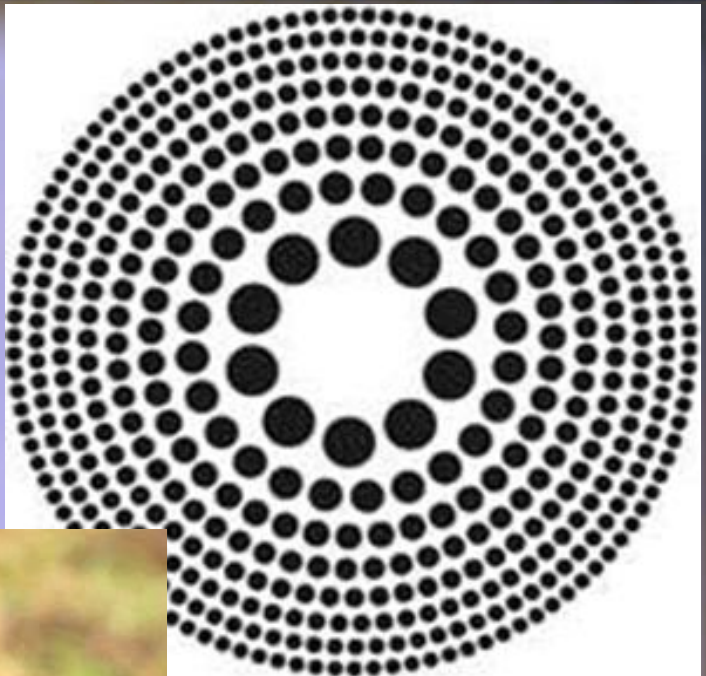

圆孔

由金属薄膜构成的纳光子结构

巴比涅原理对于纳光子结构不适用

- 既非**衍射**问题
- 亦非**夫琅禾费**远场光强度分布

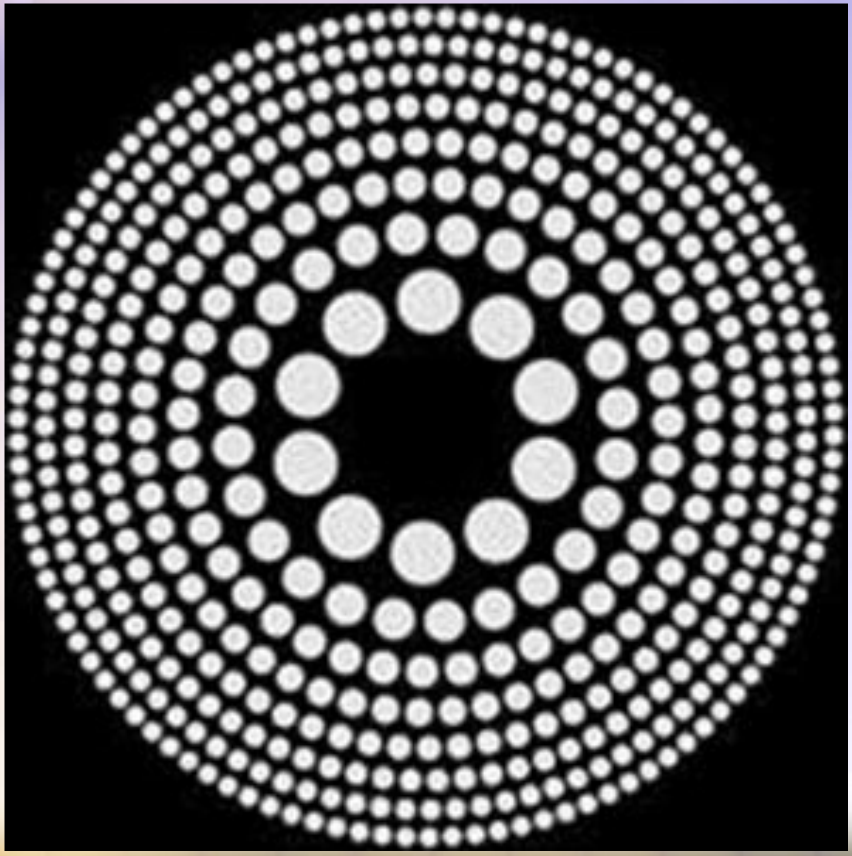

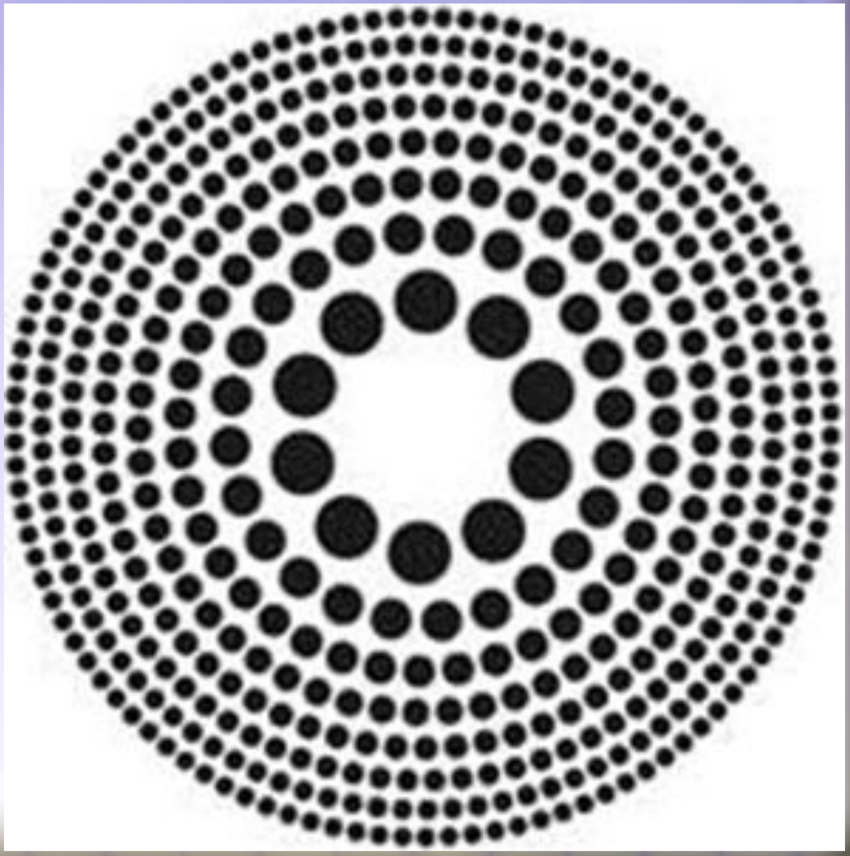

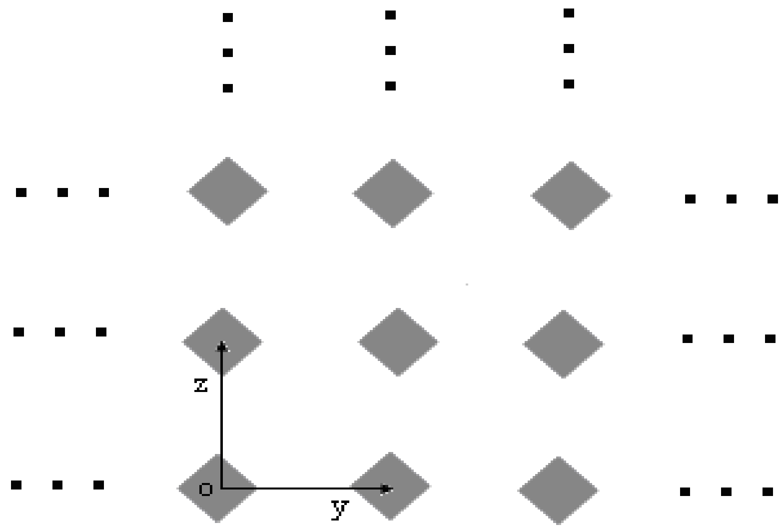
z
o
y

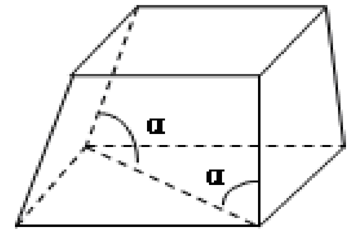
α
α

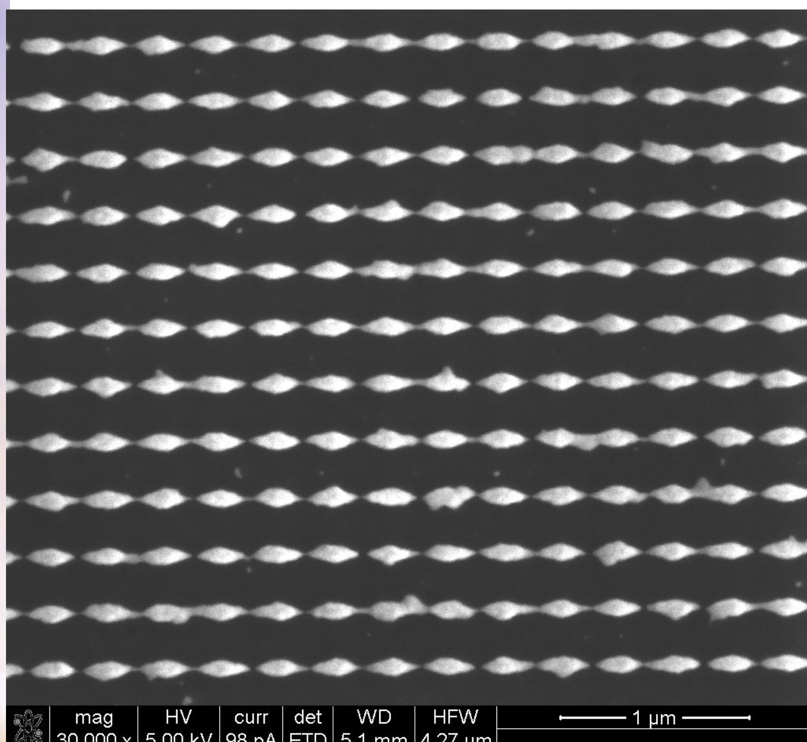
mag 30 000 x
HV 5.00 kV
curr 98 pA
det ETD
WD 5.1 mm
HFW 4.27 μm
1 μm

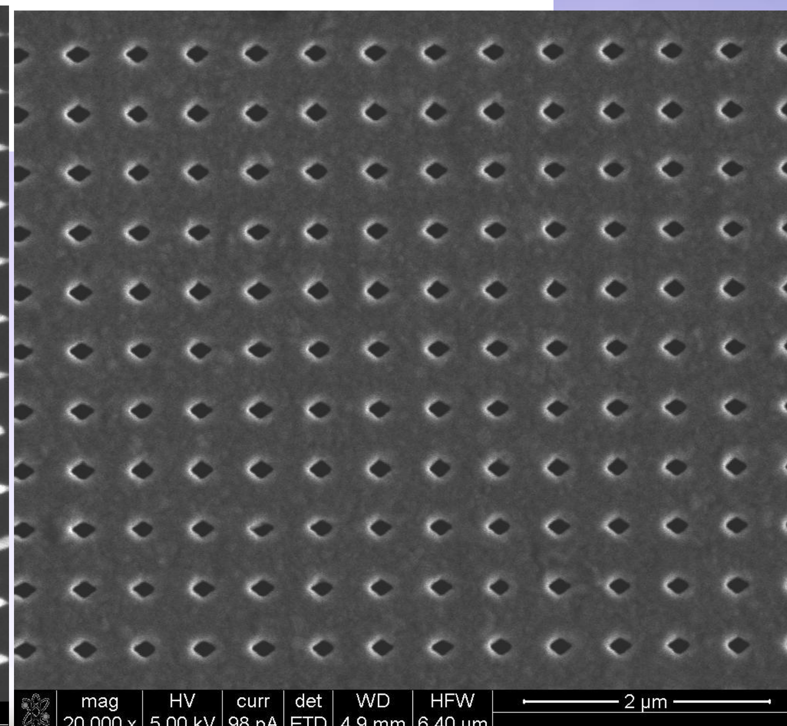
mag 20 000 x
HV 5.00 kV
curr 98 pA
det ETD
WD 4.9 mm
HFW 6.40 μm
2 μm

Contents

We are here!

- Physical mechanism of single hole
- Polarization issue of elliptical nanoholes
- Fabrication of nanohole array
- Applications of nanoholes

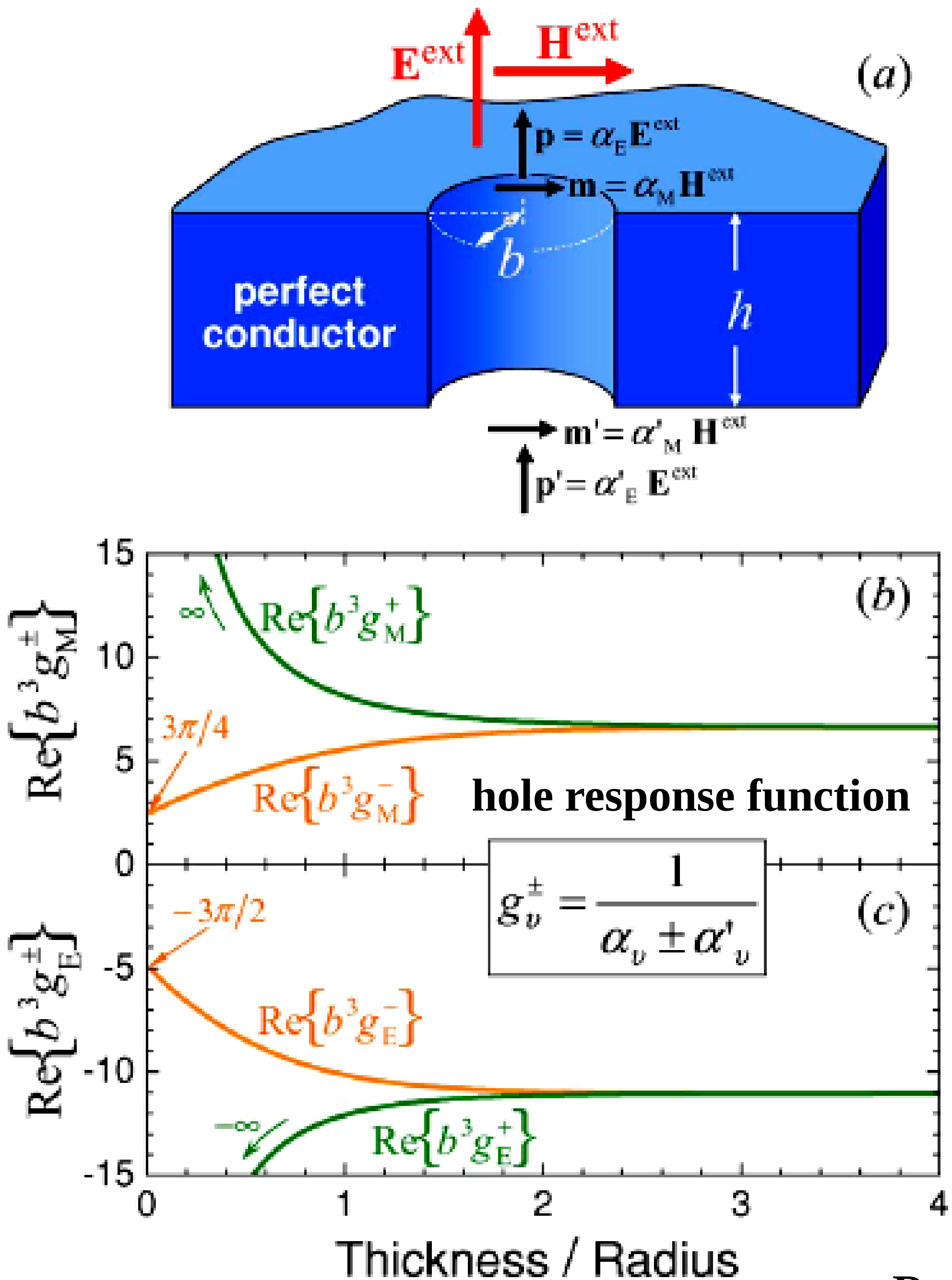

$$p = \alpha_E(E_z^{\mathrm{ext}} + G_{zz}p - Hm) + \alpha'_E(G_{zz}p' - Hm'),$$

$$p' = \alpha'_E(E_z^{\mathrm{ext}} + G_{zz}p - Hm) + \alpha_E(G_{zz}p' - Hm'),$$

$$m = \alpha_M(H_y^{\mathrm{ext}} + G_{yy}m - Hp) + \alpha'_M(G_{yy}m' - Hp'),$$

$$m' = \alpha'_M(H_y^{\mathrm{ext}} + G_{yy}m - Hp) + \alpha_M(G_{yy}m' - Hp'),$$

with a new lattice sum defined as

$$H = -ik\sum_{n\neq 0} e^{-ik_{\parallel}x_n}\partial_{x_n}\frac{e^{ikR_n}}{R_n}.$$

Review of Modern Physics 79, 1267-1290 (2007).

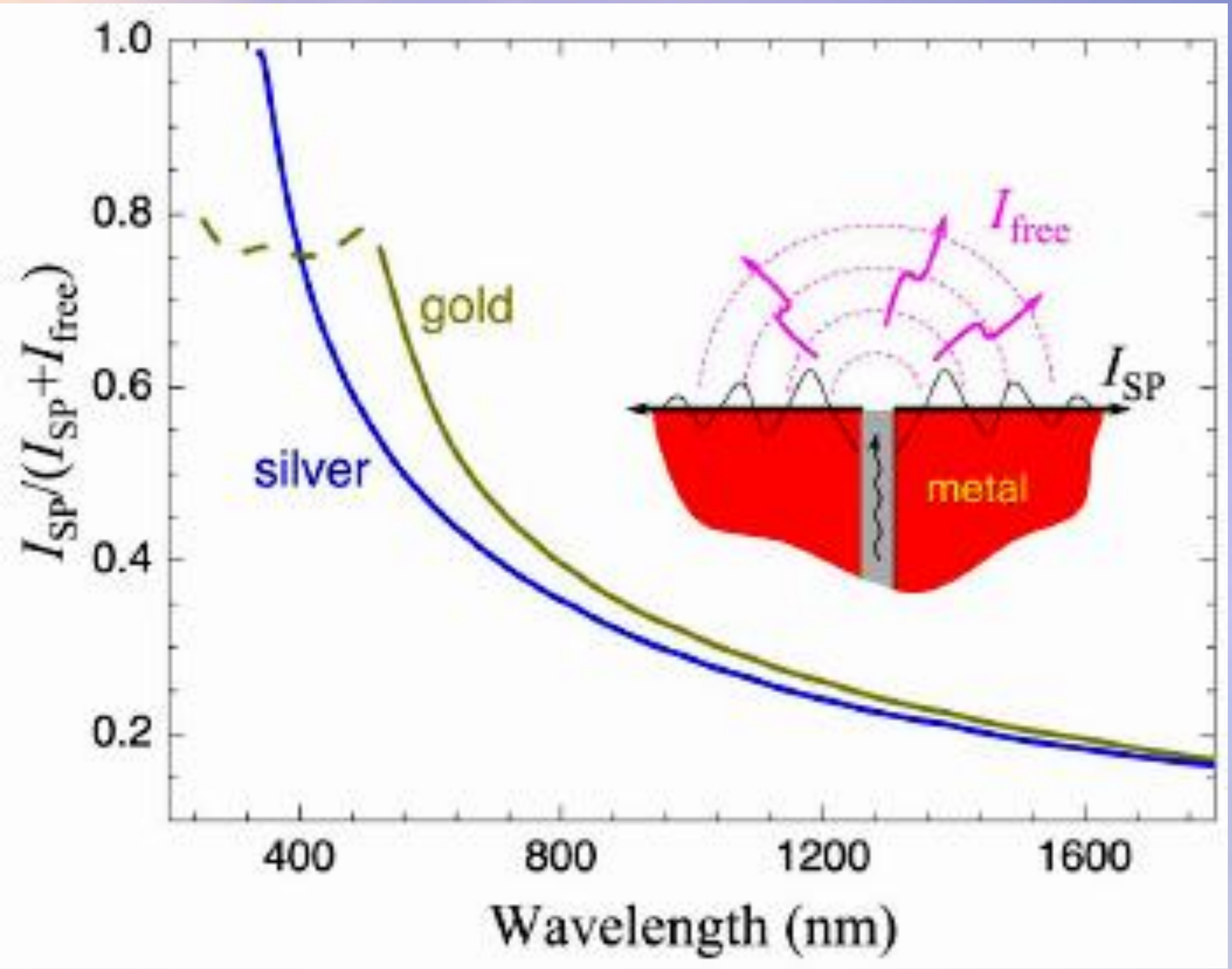

Review of Modern Physics 79, 1267-1290 (2007).

Contents

- **Physical mechanism of single hole**
- **Polarization issue of elliptical nanoholes**
- **Fabrication of nanohole array**
- **Applications of nanoholes**

We are here!

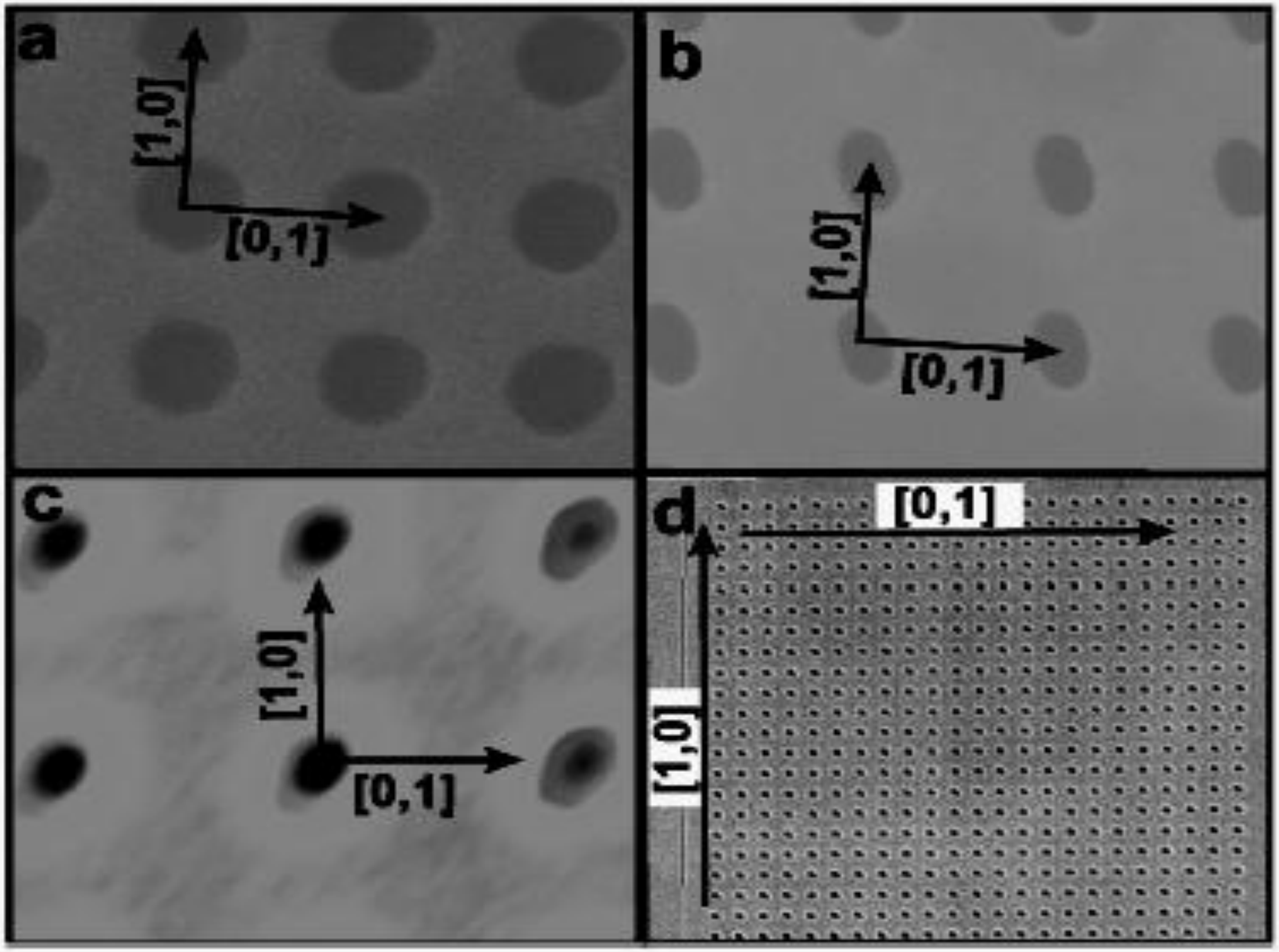

FIG. 1. Scanning electron micrographs of square nanohole arrays in gold. (a) Nearly circular holes. (b) Elliptical holes, 0.6 aspect ratio and major axis at $-12°$ to the [1, 0]. (c) Elliptical holes, 0.6 aspect ratio and major axis at $33°$ to the [1, 0] axis. (d) An expanded view of (c) showing the full 16.1 μm wide array of 529 holes (holes spaced by 704 nm).

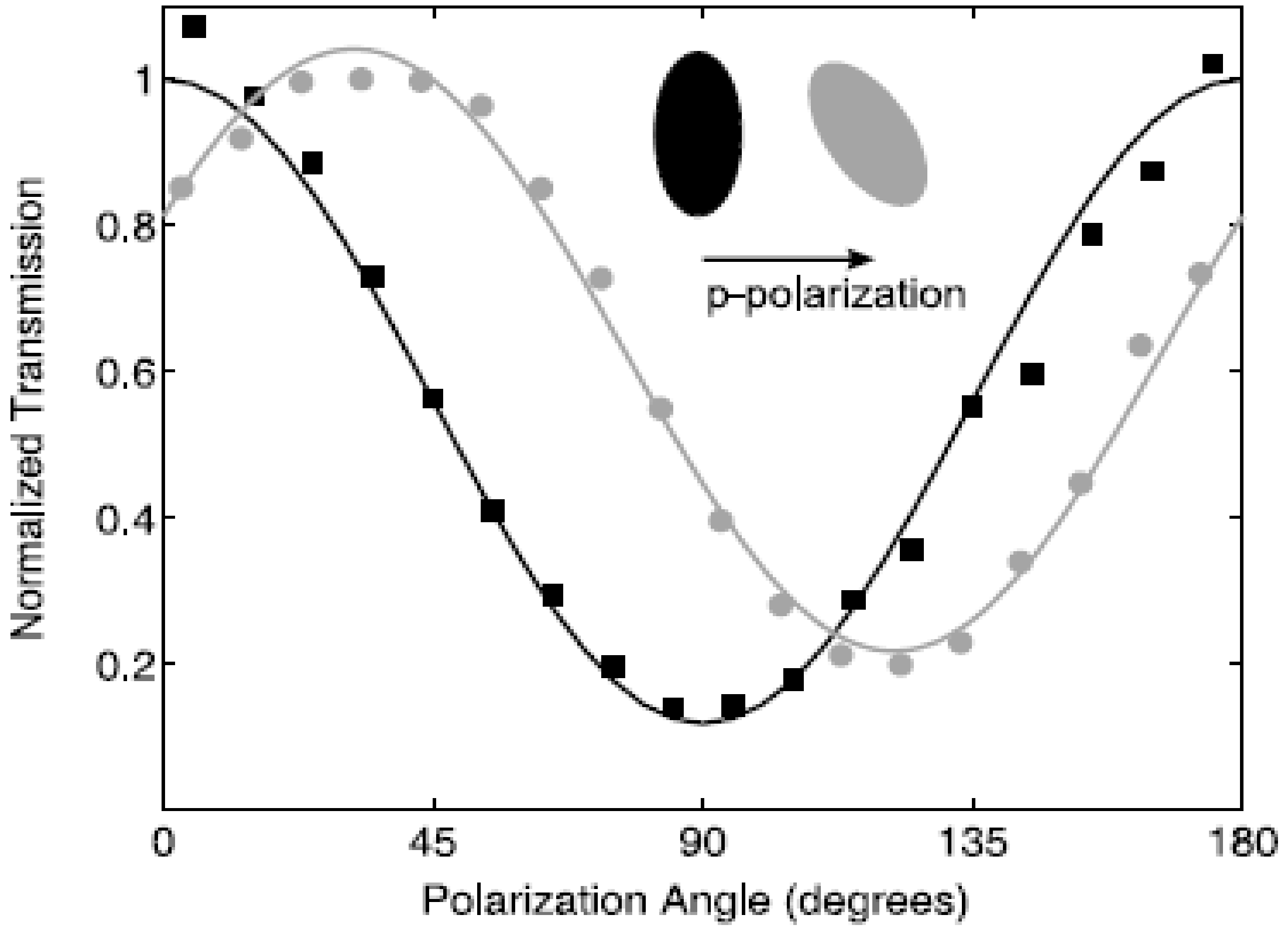

FIG. 3. Polarization dependence of transmission at the (0, 1) resonance peak, normalized to the maximum. Transmission shows cosine dependence when the major axis of the ellipse is oriented both at 0° and 33° to the [1, 0] axis of the array. The *p* polarization, along the [0, 1] direction of the lattice, corresponds to a polarization angle of zero degrees. The maximum transmission occurs for polarization perpendicular to the broad side of the ellipse.

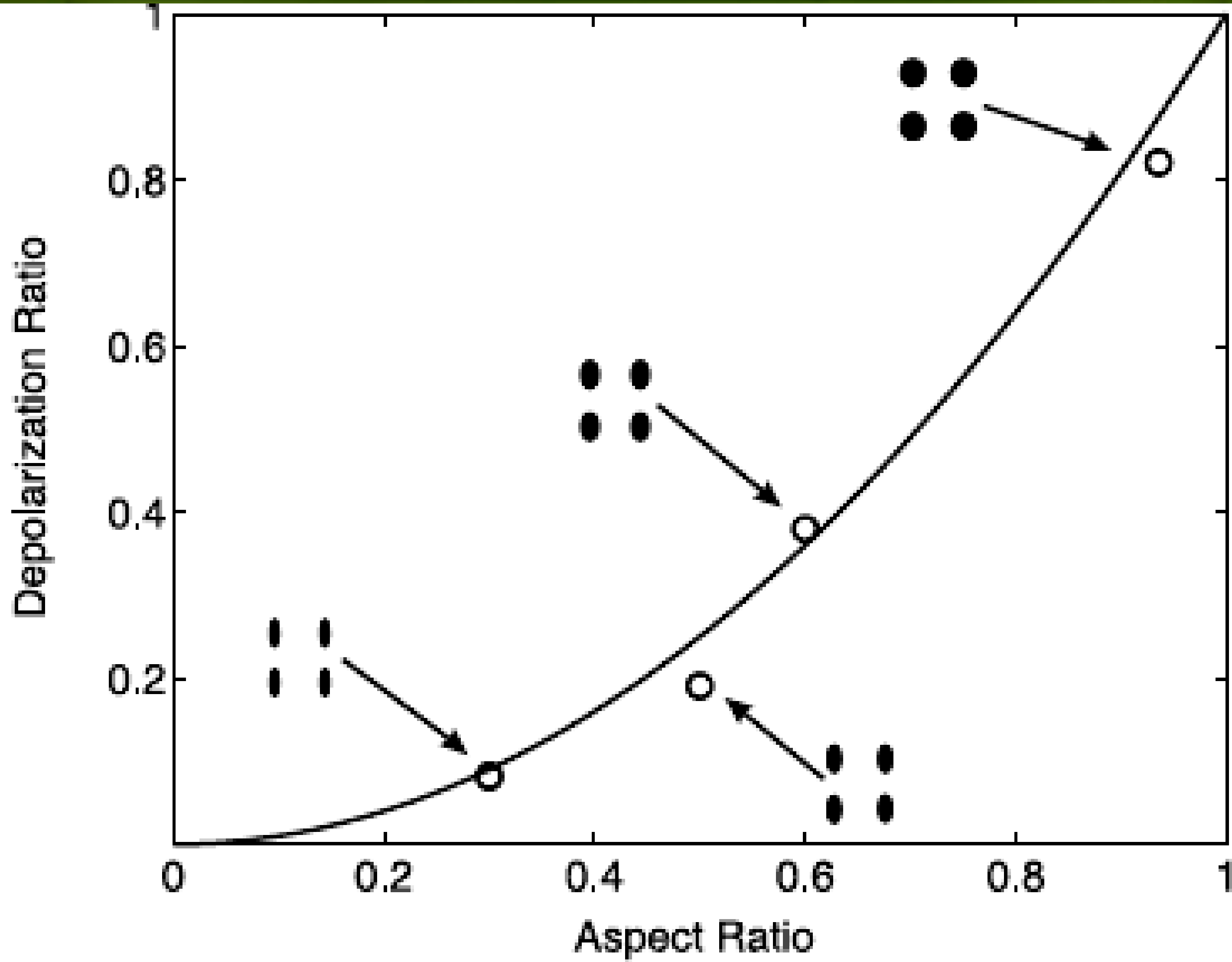

FIG. 4. The depolarization ratio of the transmitted light as a function of the aspect ratio of the holes. Solid line shows the $y = x^2$ curve.

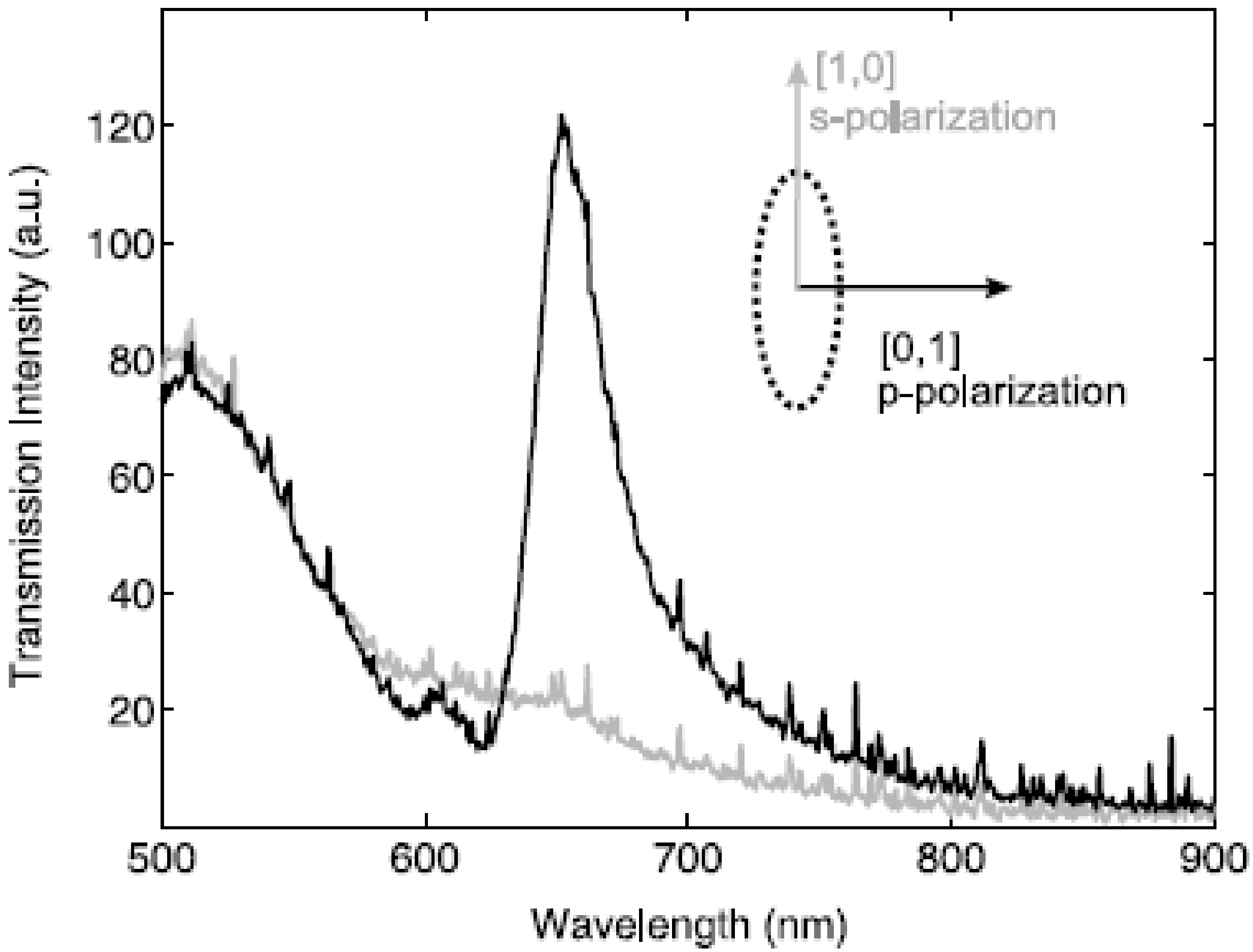

FIG. 2. Transmission spectrum through elliptical nanohole array for two orthogonal linear polarizations, with a 0.3 aspect ratio between the minor and major axes of the ellipse. The p polarization is parallel to the $[0, 1]$ direction.

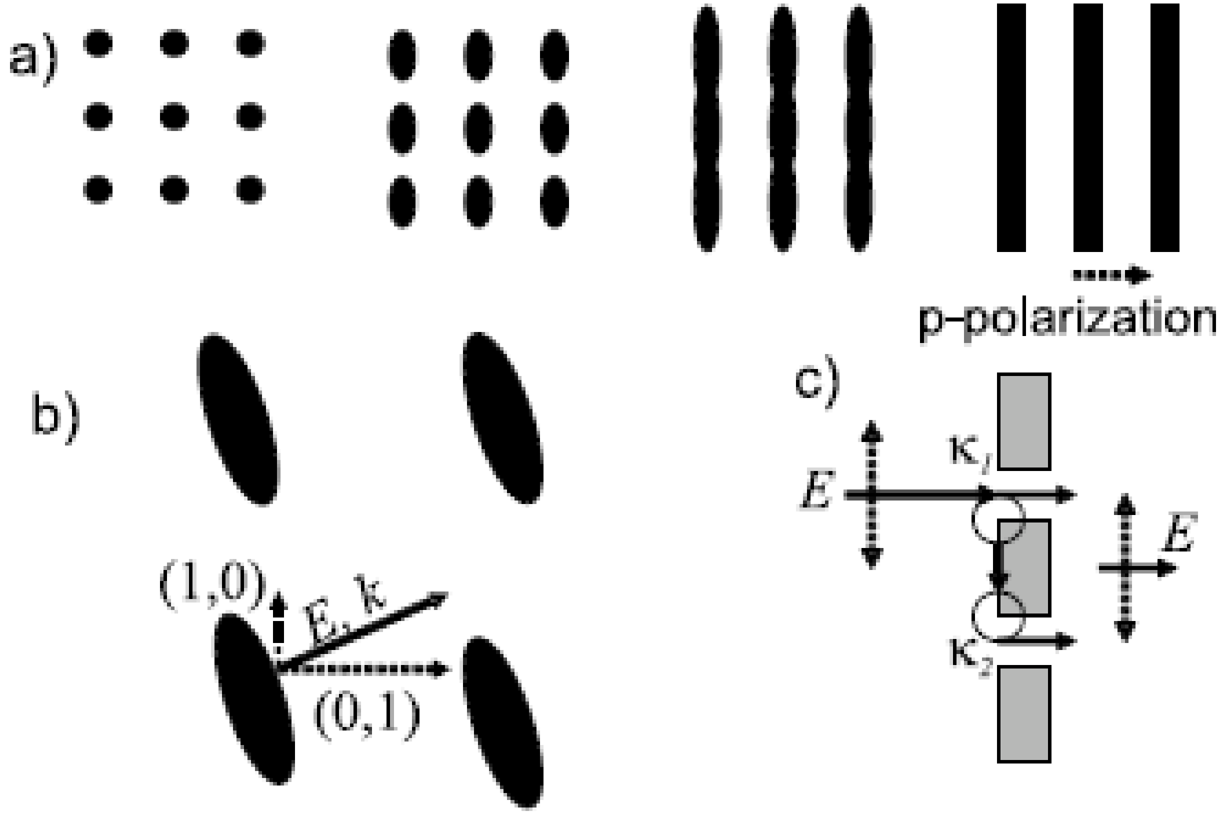

FIG. 5. (a) Elliptical holes approaching limiting case of slits, which only show enhanced transmission for *p* polarized light. (b) Enhanced SP excitation perpendicular to major axis of ellipse leads to preferential excitation of the (0, 1) resonance with respect to the (1, 0) resonance. (c) Coupling both into and out of the SP mode is required to obtain enhanced transmission from periodic array of holes, which results in a squared dependence of the enhanced transmission on the coupling strength.

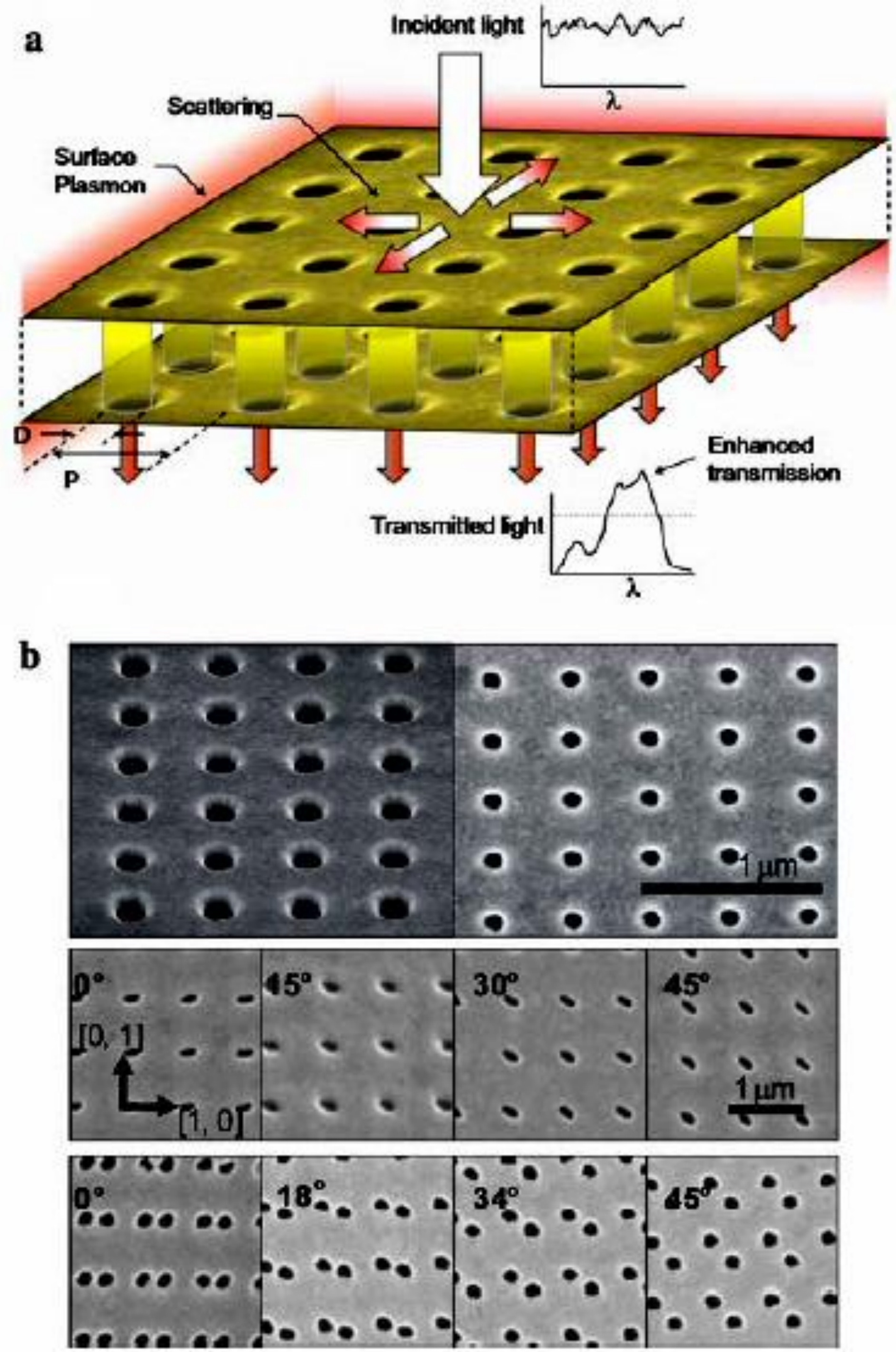

Equal period in X- and Y-axis

$$\lambda^{\mathrm{SP}}(i,j) = p\left(i^2 + j^2\right)^{-1/2}\left(\frac{\varepsilon_d \varepsilon_m}{\varepsilon_d + \varepsilon_m}\right)^{1/2}$$

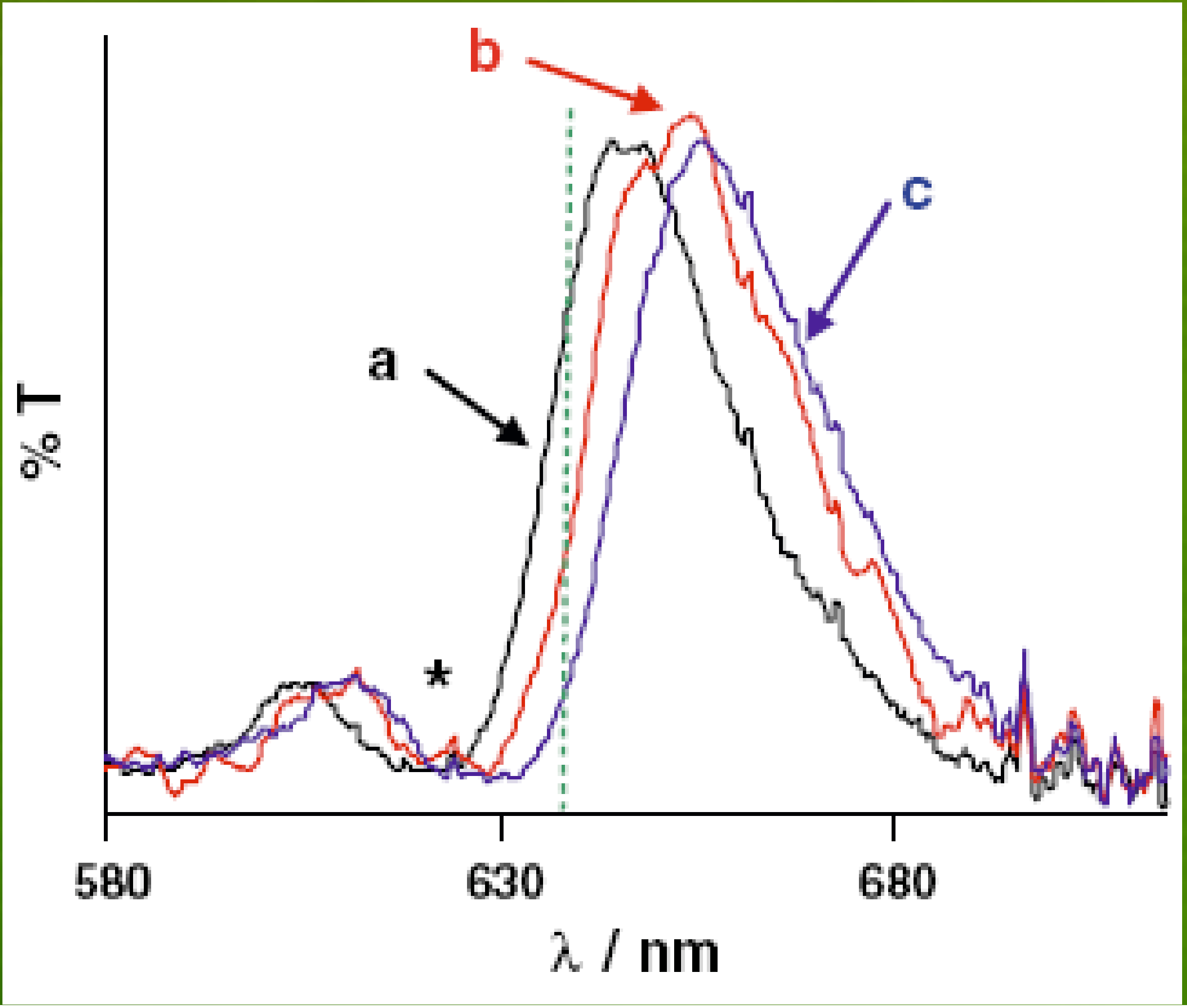

a bare gold surface; b gold with monolayer of MUA; and c gold-MUA layer with BSA.

Polarization dependent of biaxial nanoholes

Unequal periods: a, b

a>b

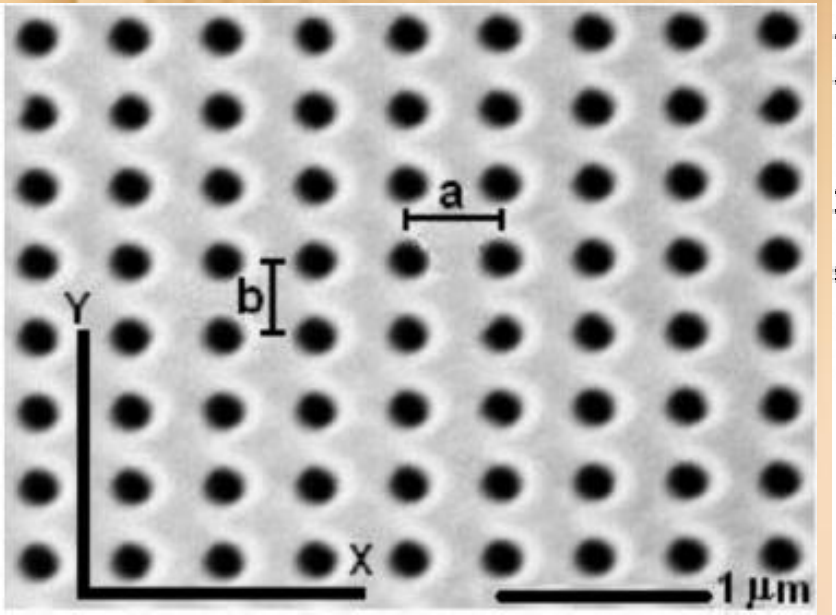

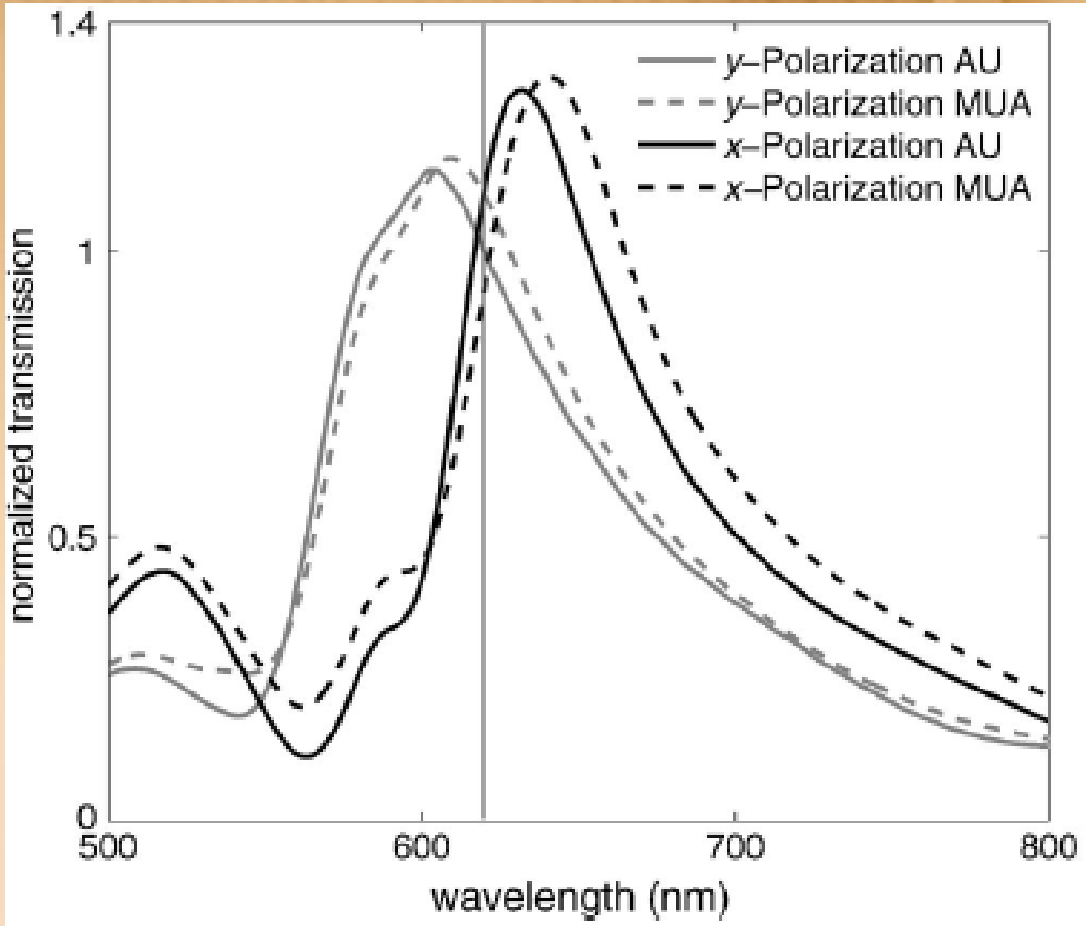

$$\lambda_{max}(i,j) = \frac{ab}{\sqrt{i^2b^2 + j^2a^2}}\sqrt{\frac{\varepsilon_d\varepsilon_m}{\varepsilon_d + \varepsilon_m}}.$$

Strong Influence of Hole Shape on Extraordinary Transmission

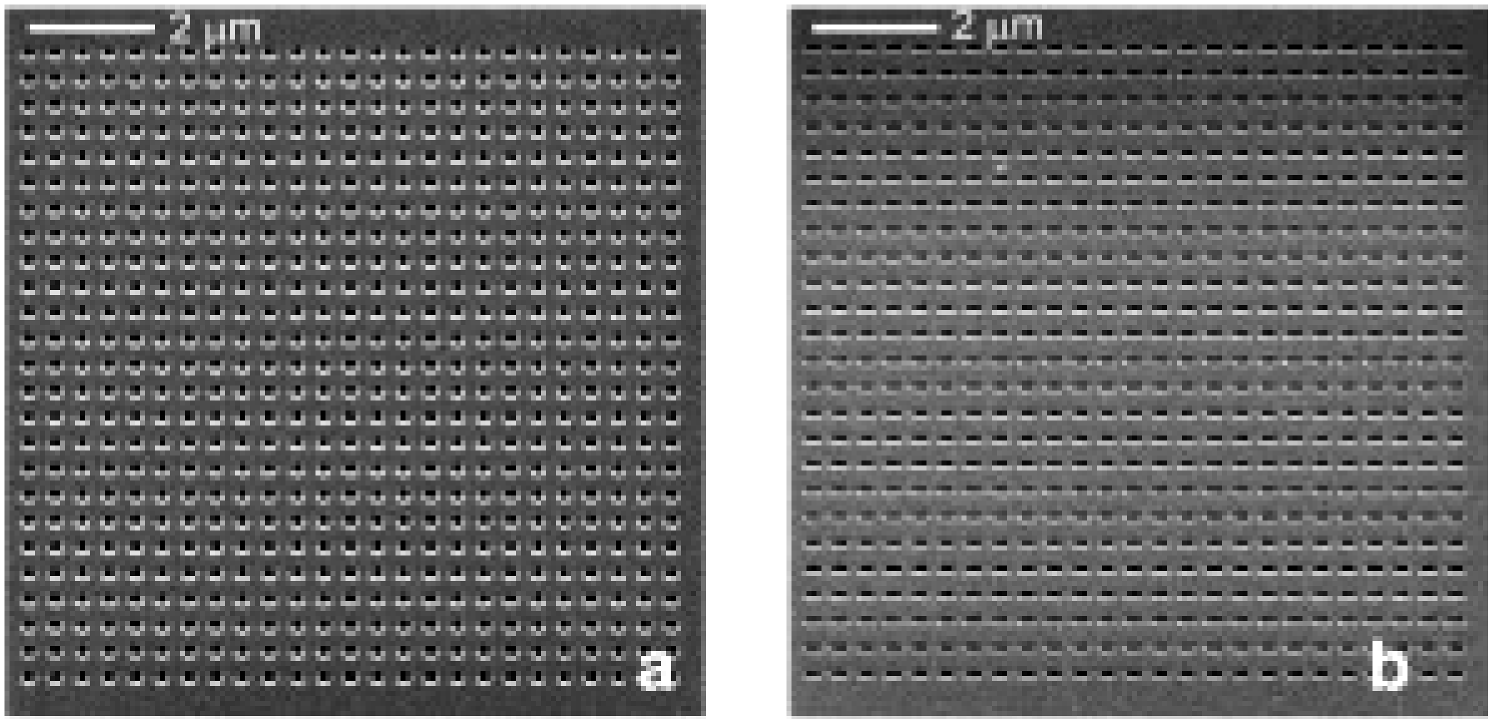

FIG. 1. Focused ion beam images of two periodic subwavelength hole arrays fabricated in a 200 nm thick gold film. Both arrays have a period of 425 nm. (a) An array consisting of circular holes with a diameter of 190 nm. (b) An array consisting of rectangular holes of 75×225 nm^2.

PRL,92, 183901(2004)

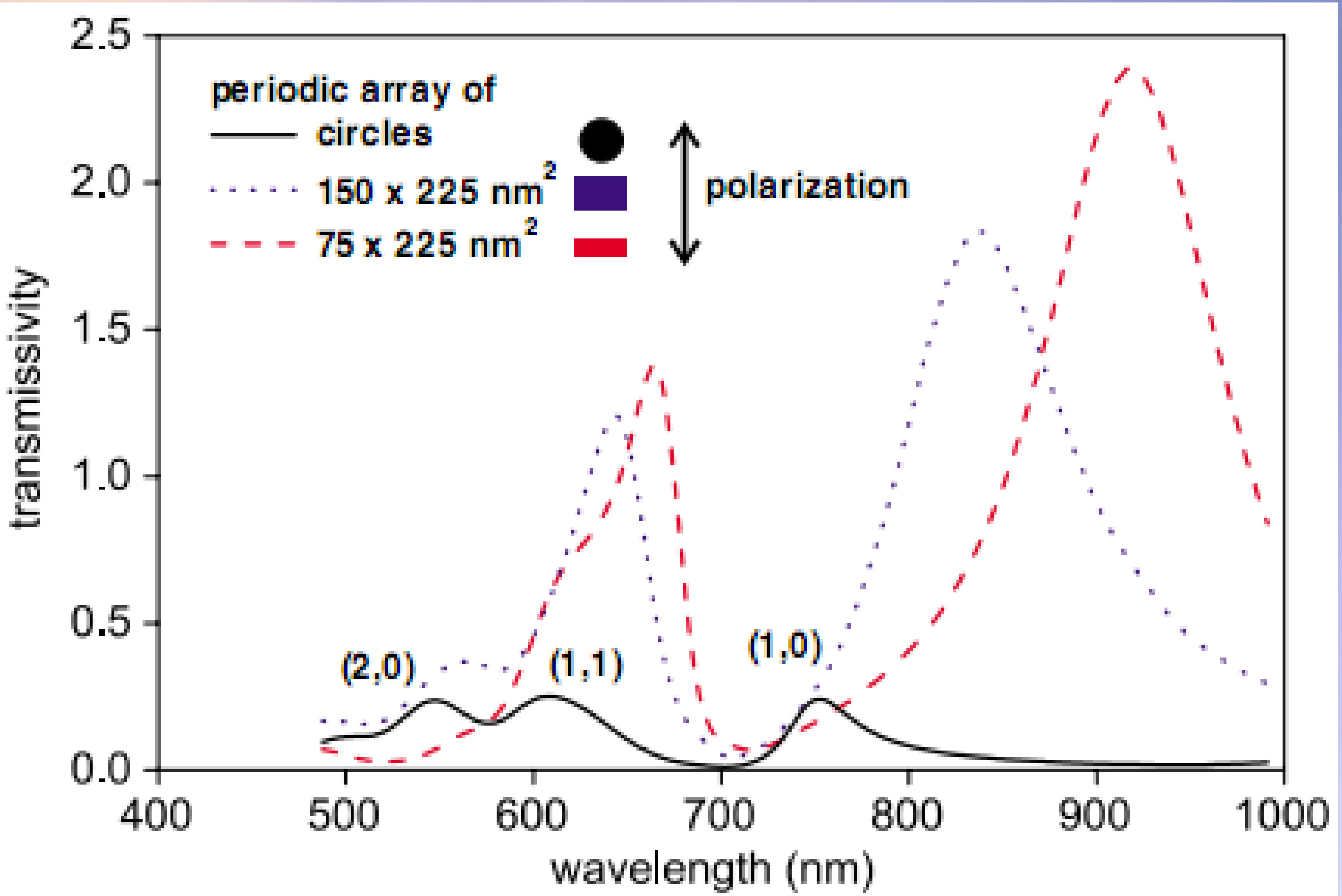

periodic array of
circles
150 x 225 nm²
75 x 225 nm²
polarization
(2,0)
(1,1)
(1,0)
transmissivity
wavelength (nm)
0.0
0.5
1.0
1.5
2.0
2.5
400
500
600
700
800
900
1000

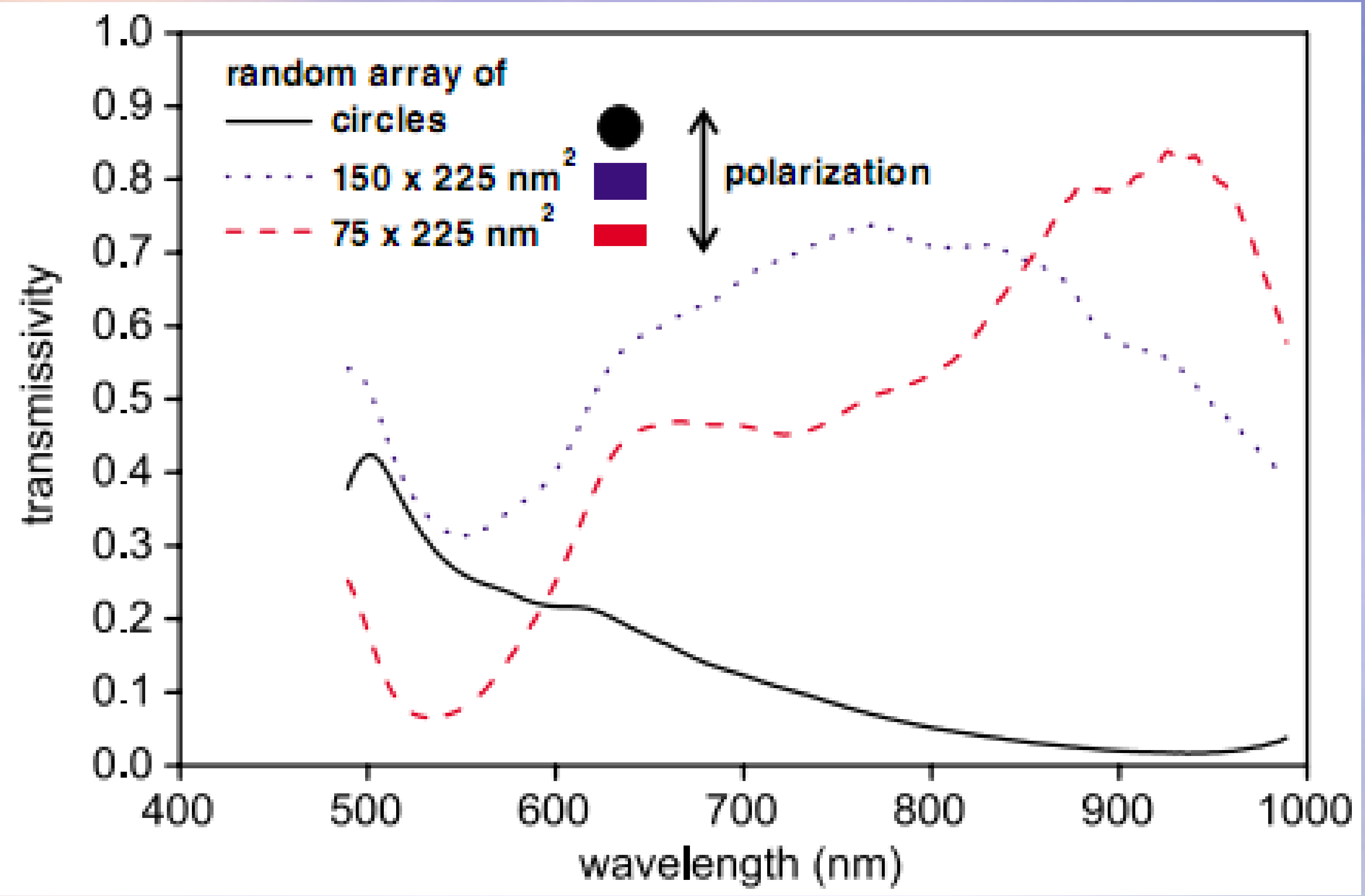

random array of
circles
150 x 225 nm²
75 x 225 nm²
polarization
transmissivity
1.0
0.9
0.8
0.7
0.6
0.5
0.4
0.3
0.2
0.1
0.0
400
500
600
700
800
900
1000
wavelength (nm)

Contents

- Physical mechanism of single hole
- Polarization issue of elliptical nanoholes
- **Fabrication of nanohole array**
- Applications of nanoholes

We are here!

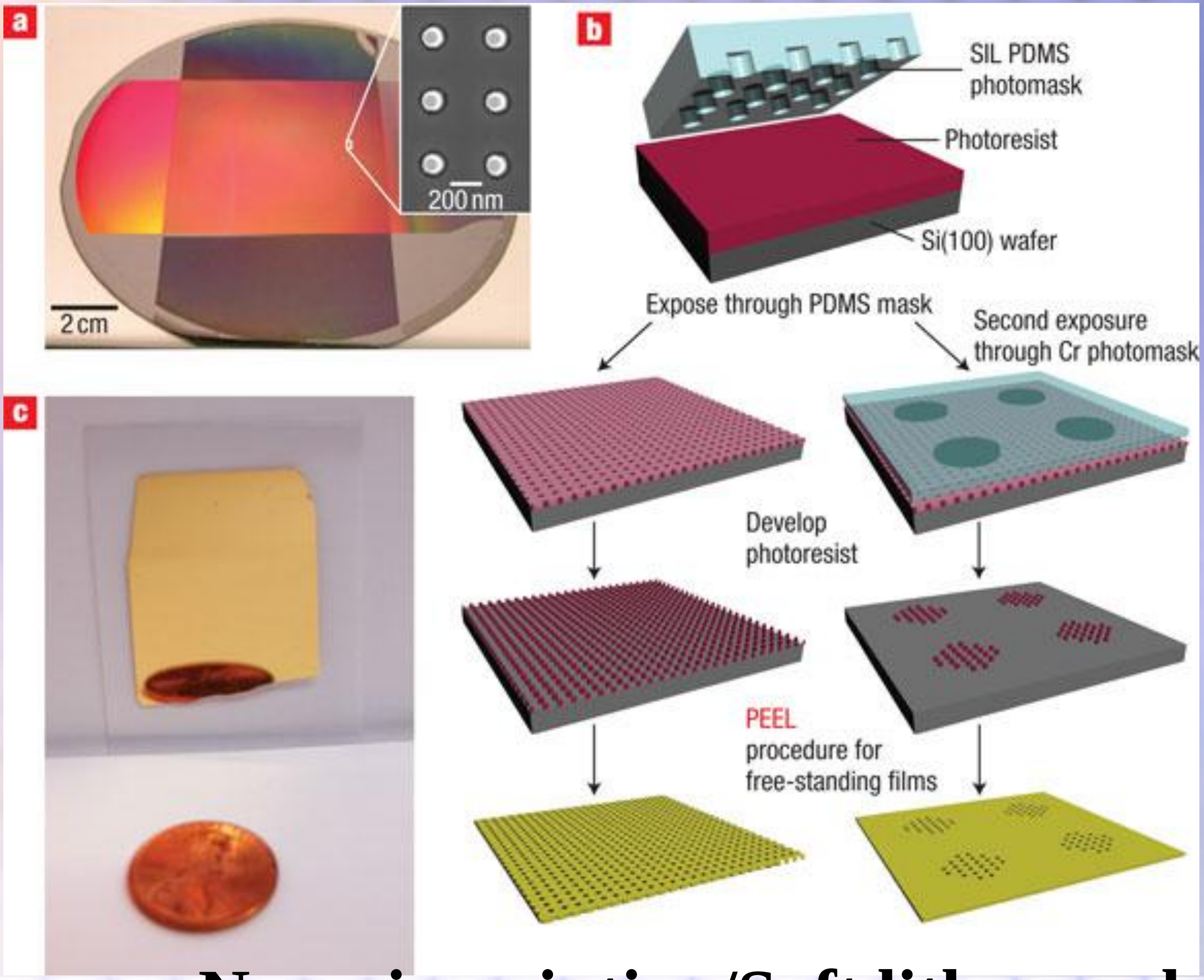

Nano-imprinting/Soft lithography

Fabrication of Nanoholes array

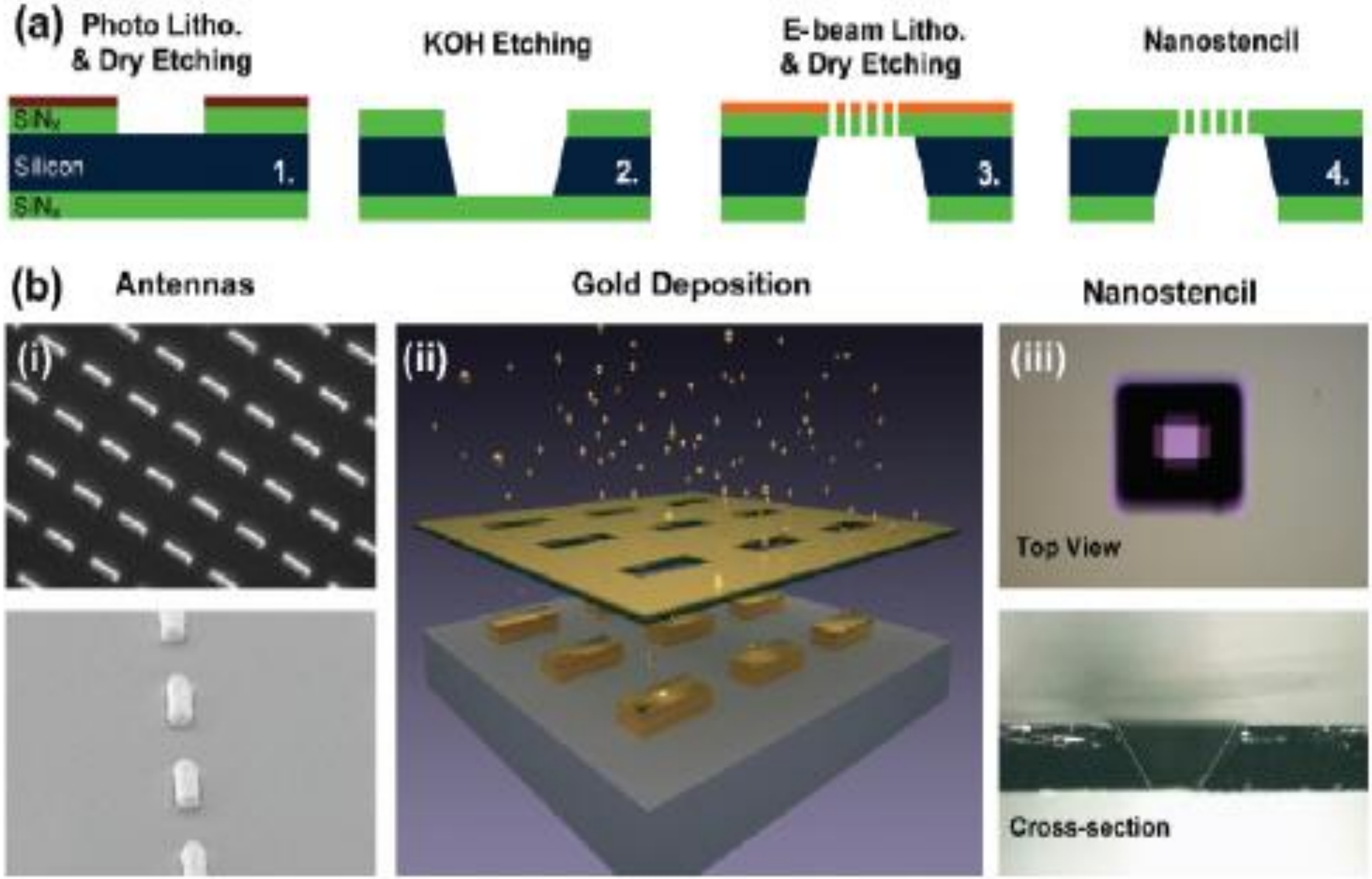

Three optional methods

E-beam lithography

/focused ion beam

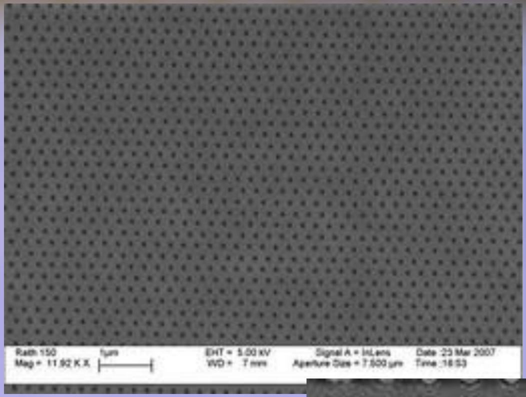

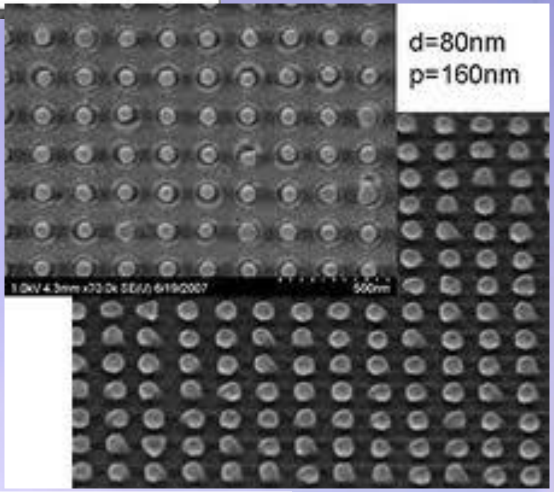

Laser interference lithography

Self-assembly monolayer

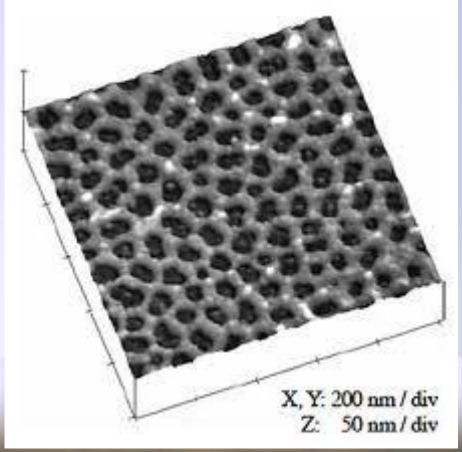

Contents

- Physical mechanism of single hole
- Polarization issue of elliptical nanoholes
- Fabrication of nanohole array
- **Applications of nanoholes**

We are here!

Optical trapping with nanoholes

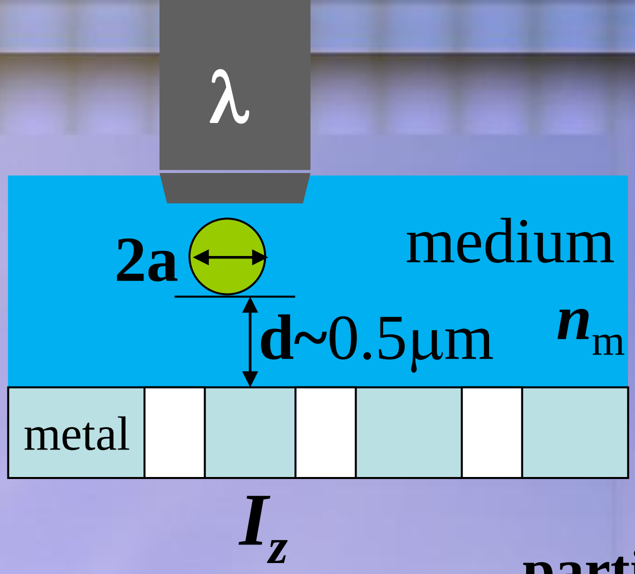

Manipulation target:

- **cells, virus, DNA**
- **non-biological particles in fluidic**

particle

$$m = \frac{n_p}{n_m}$$

Critical trapping distance from the surface, *d*

metal

I_{SPP}

$$d = \frac{\lambda}{4\pi}\sqrt{\frac{n_m^2+\varepsilon_m}{-n_m^4}}\ln\left(\frac{3\lambda^3}{16\pi^3 a^3}\frac{n_m}{\sqrt{-(n_m^2+\varepsilon_m)}}\frac{m^2+2}{m^2-1}\frac{I_x(0)}{I_z}\right)$$

medium

I_{hole}

where λ is the wavelength of the light source, n_m is the refractive index of the medium in which the particles are suspended, ε_m is the real part of the dielectric constant of the metal, a is the particle radius, $m = \frac{n_p}{n_m}$ is the refractive index contrast, with n_p being the refractive index of the particle, $I_x(0)$ is the surface plasmon intensity at the surface of the metal, and I_z is the intensity of the transmitted light through the nanoholes. If the surface plasmon intensity is slightly higher than the transmitted light intensity, a trapping distance of 0.5 μm may be obtained

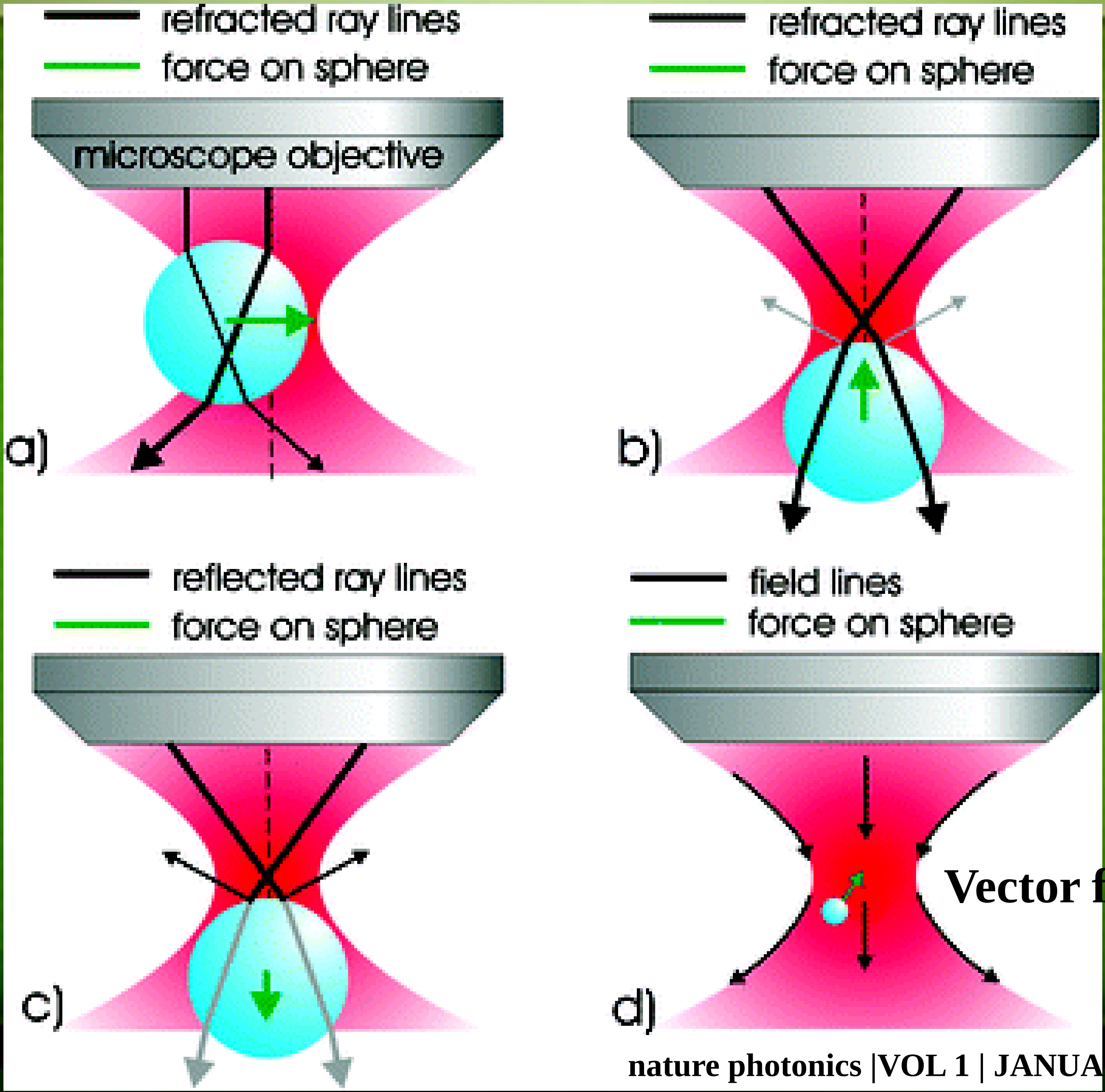

Vector field

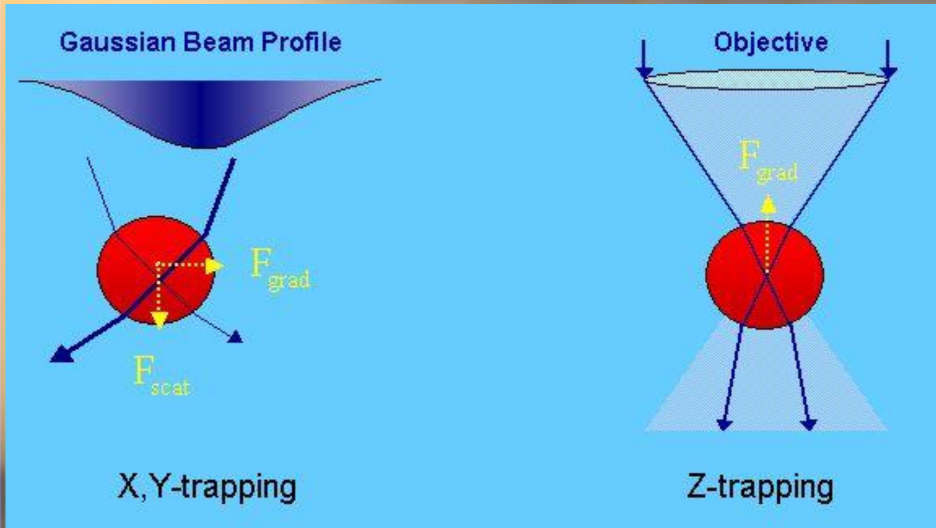

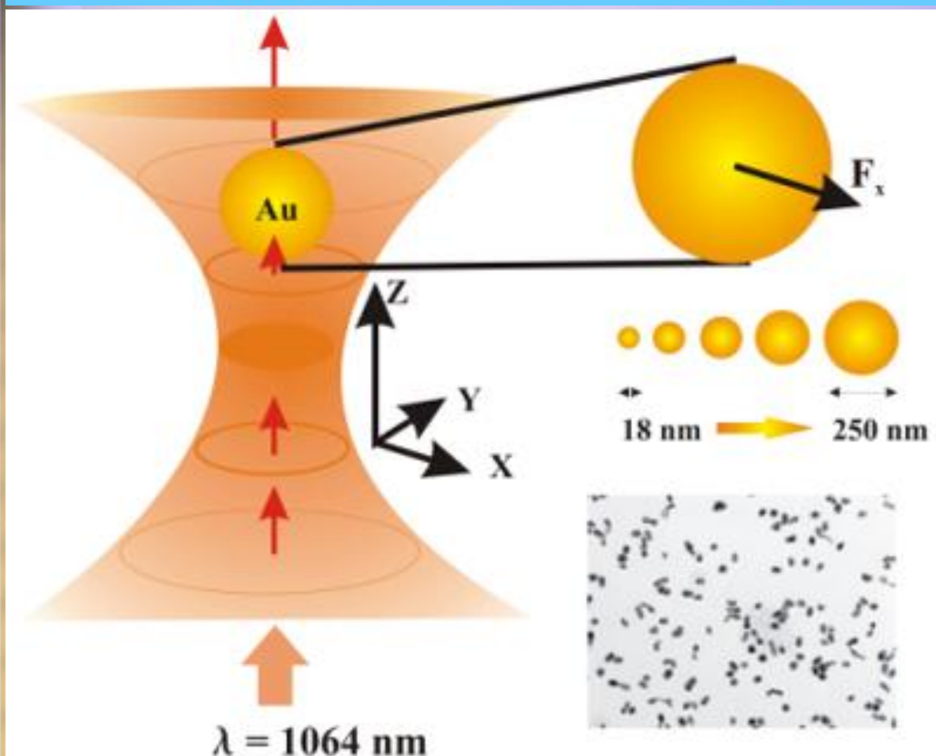

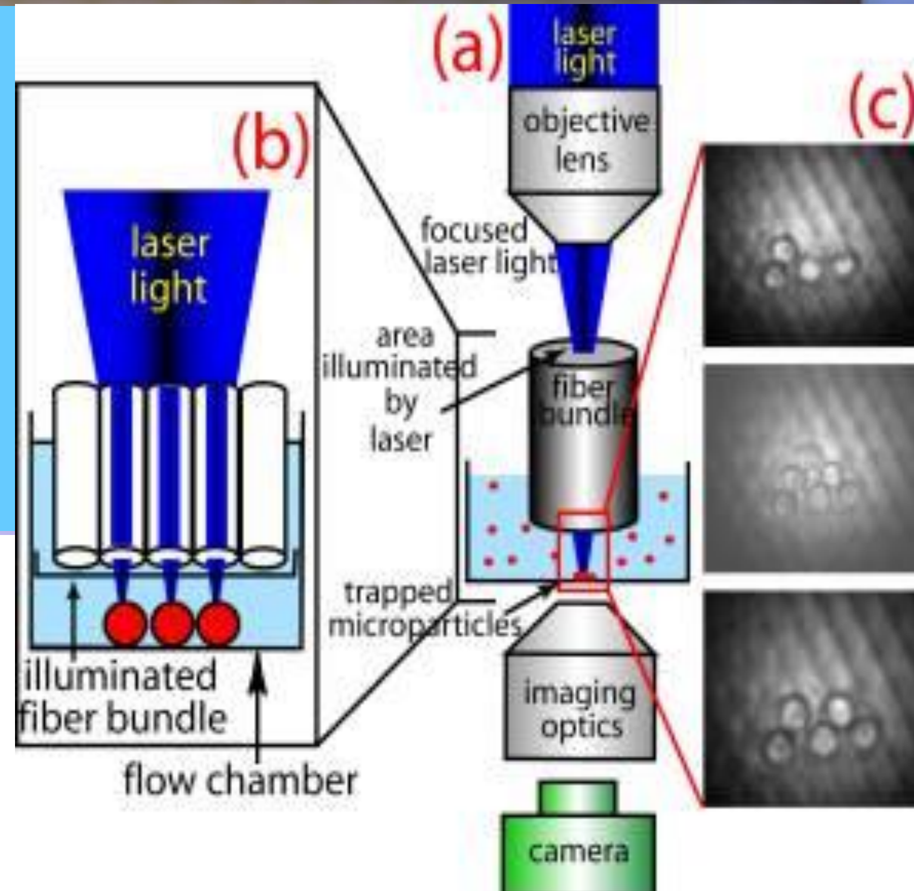

Optical trapping of gold nanoparticles

Practical plasmonic crystal biosensors

Images and schematic illustrations of a quasi-3D plasmonic crystal. (A) SEM of a crystal. (Upper Inset) A low-resolution optical image illustrating the diffraction colors produced by these structures. (Lower Inset) A high-magnification SEM that shows the upper and lower levels of gold. (B) Schematic illustration of the normal incidence transmission mode geometry used to probe these devices. The intensity of the undiffracted, transmitted light is monitored across the UV, visible, and near-infrared regions of the spectrum. (Inset) A close-up schematic illustration of the crystal.

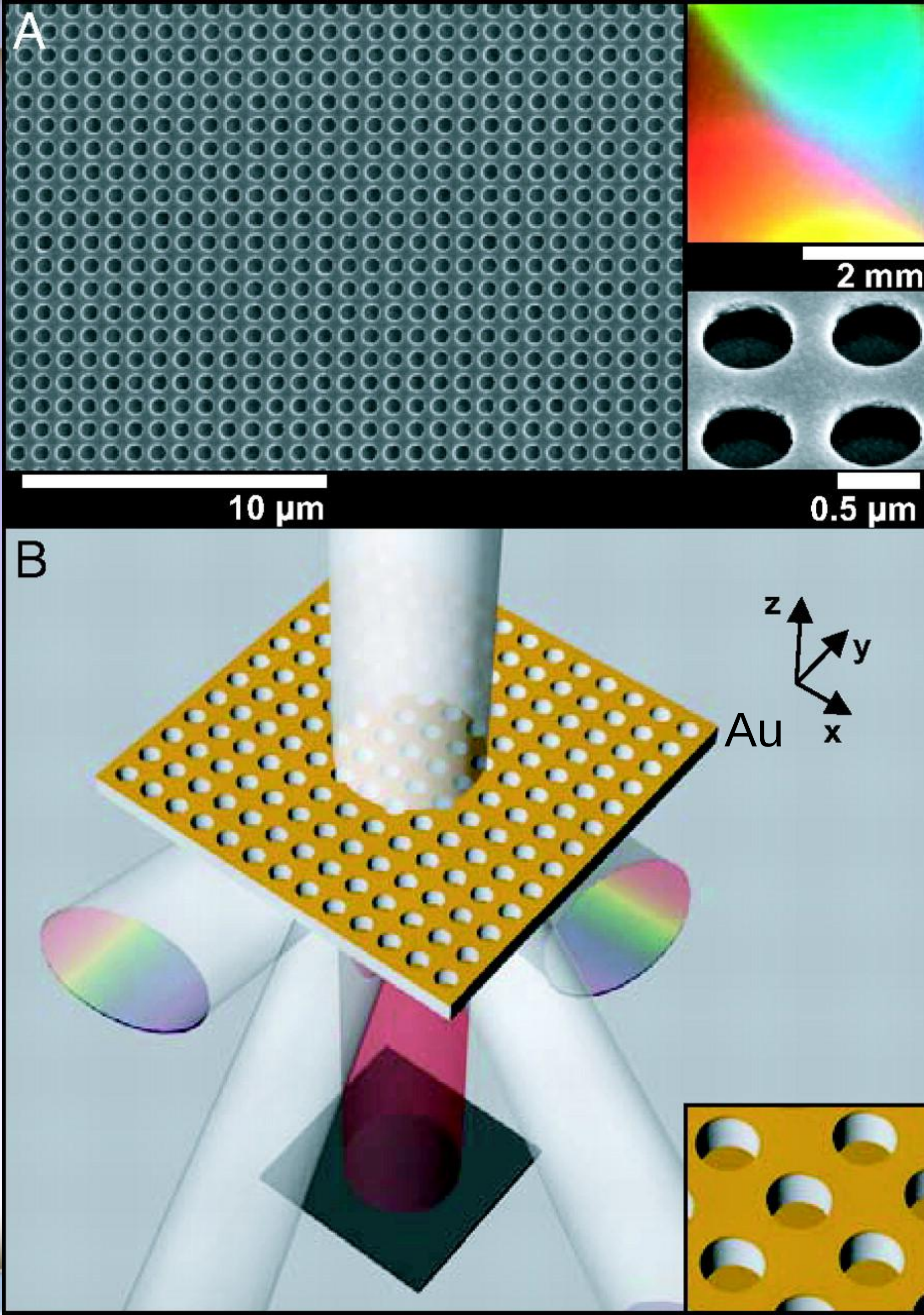

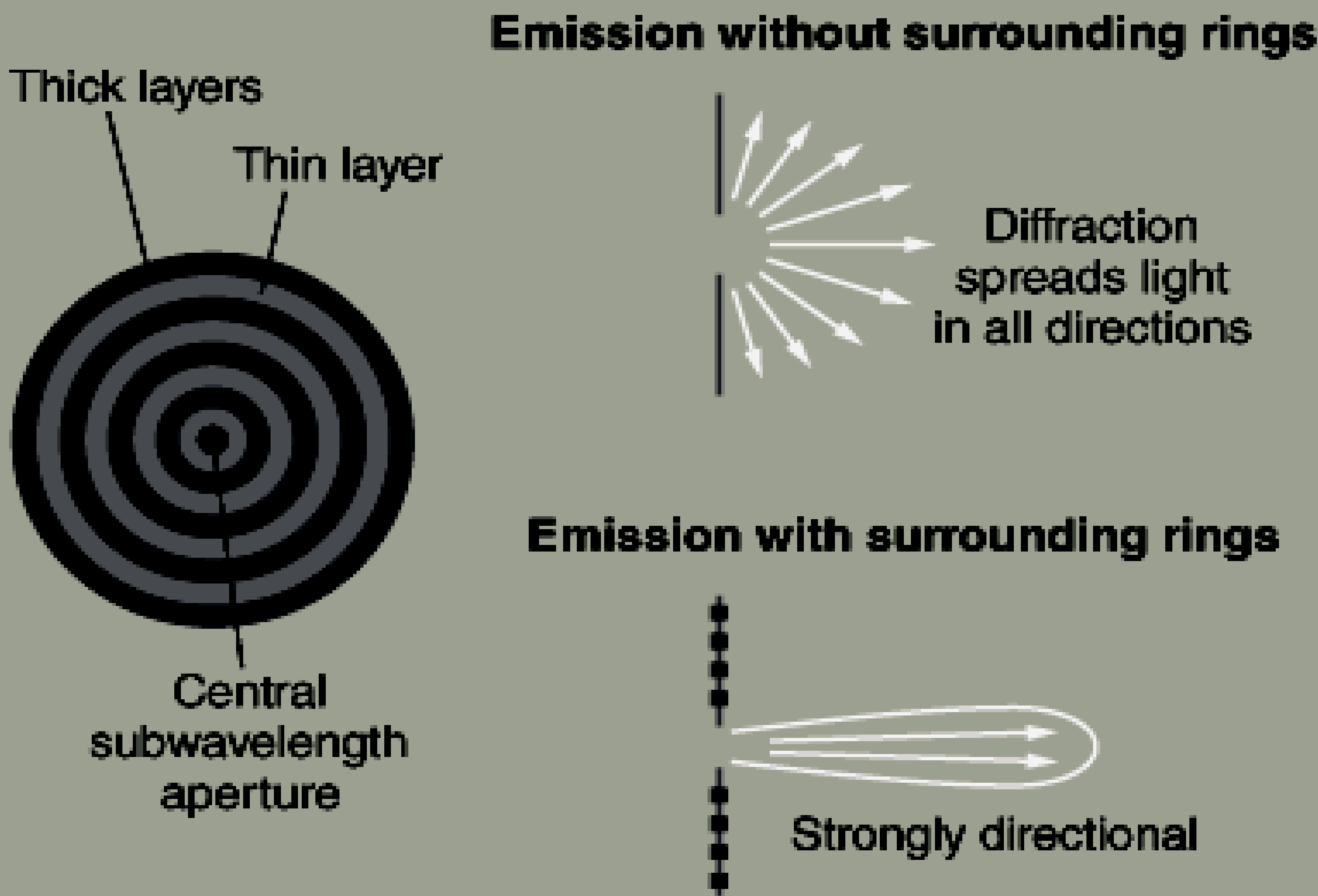
Thick layers
Thin layer
Central subwavelength aperture
Emission without surrounding rings
Diffraction spreads light in all directions
Emission with surrounding rings
Strongly directional

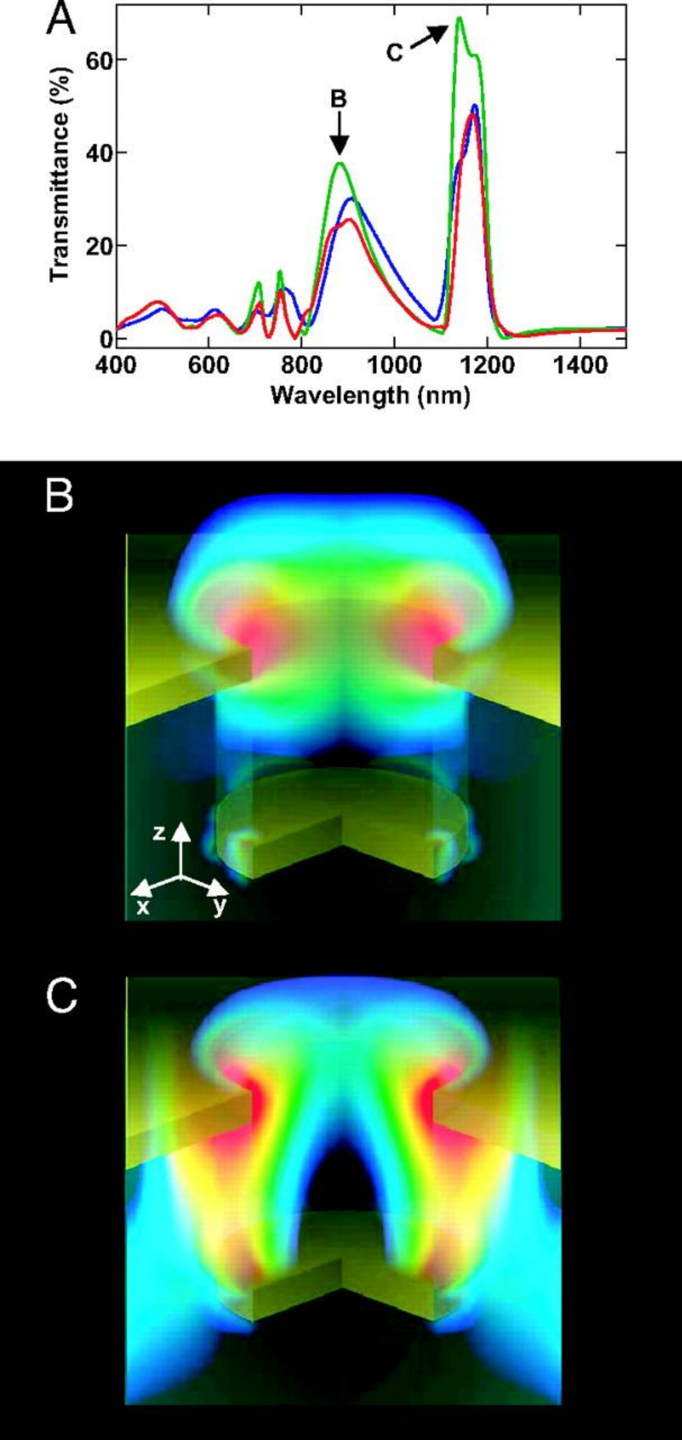

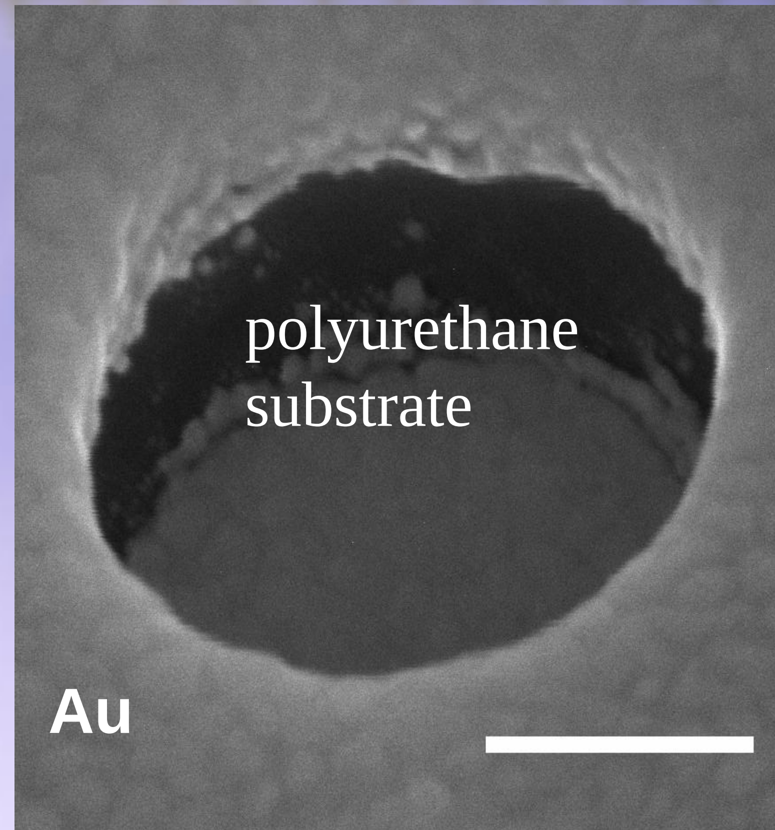

The SPR effects were produced on the nanoscale holes in the Au film and on the separate Au disks at the bottoms of the wells.

http://www.nersc.gov/news/science/plasmonic.php

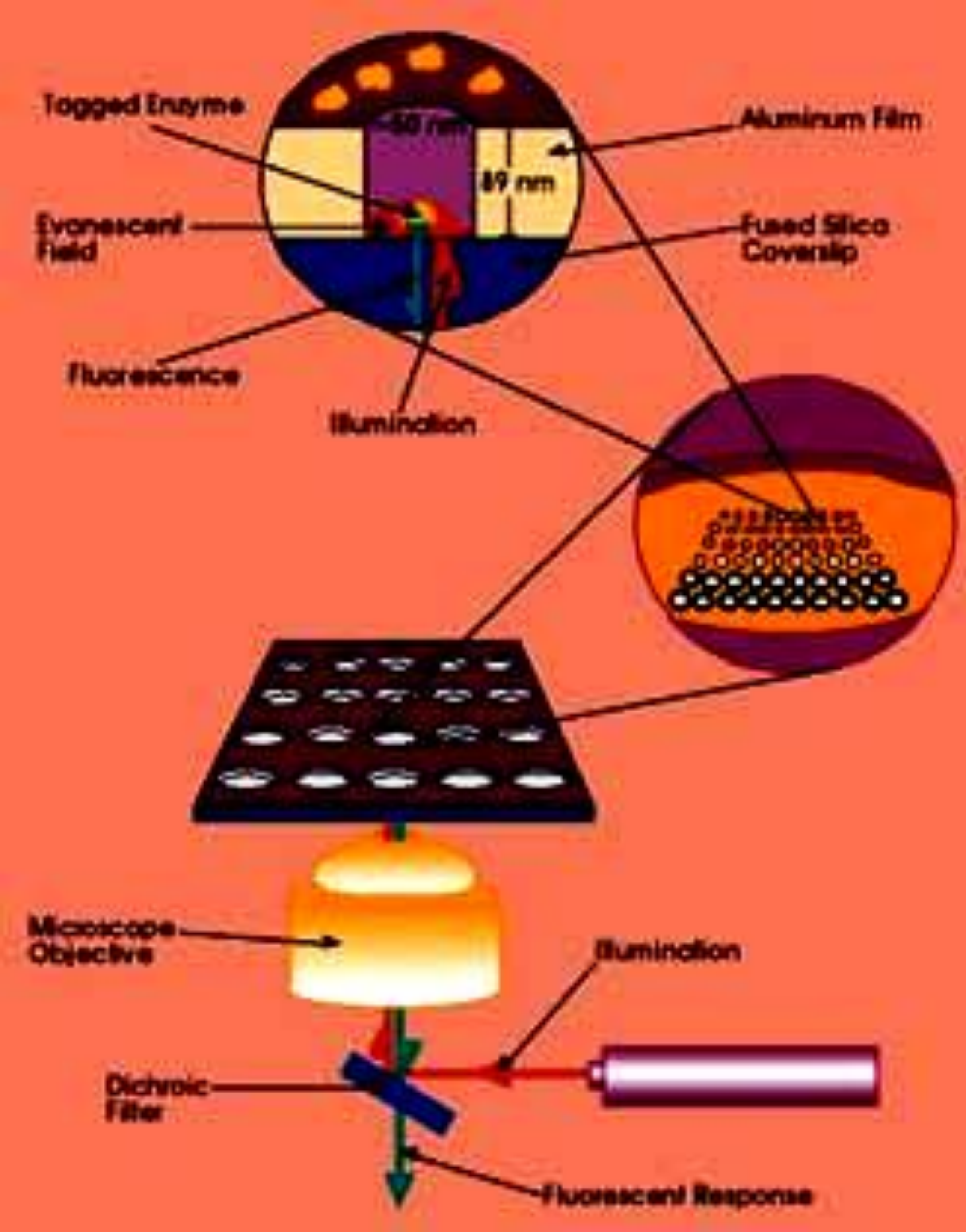

Nanoholes Improve Single-Molecule Analysis

Subwavelength holes in an Al film enable researchers to **observe the dynamics of single molecules** at more realistic concentrations. **The holes act as zero-mode waveguides**, permitting the excitation light for fluorescence correlation spectroscopy to enter into the sample chamber as an evanescent field so that **only one molecule near the opening may be stimulated**. The arrays of holes are chemically isolated on the chip, allowing the user to perform multiple experiments simultaneously.

Surface Plasmon–Quantum Dot Coupling from Arrays of Nanoholes

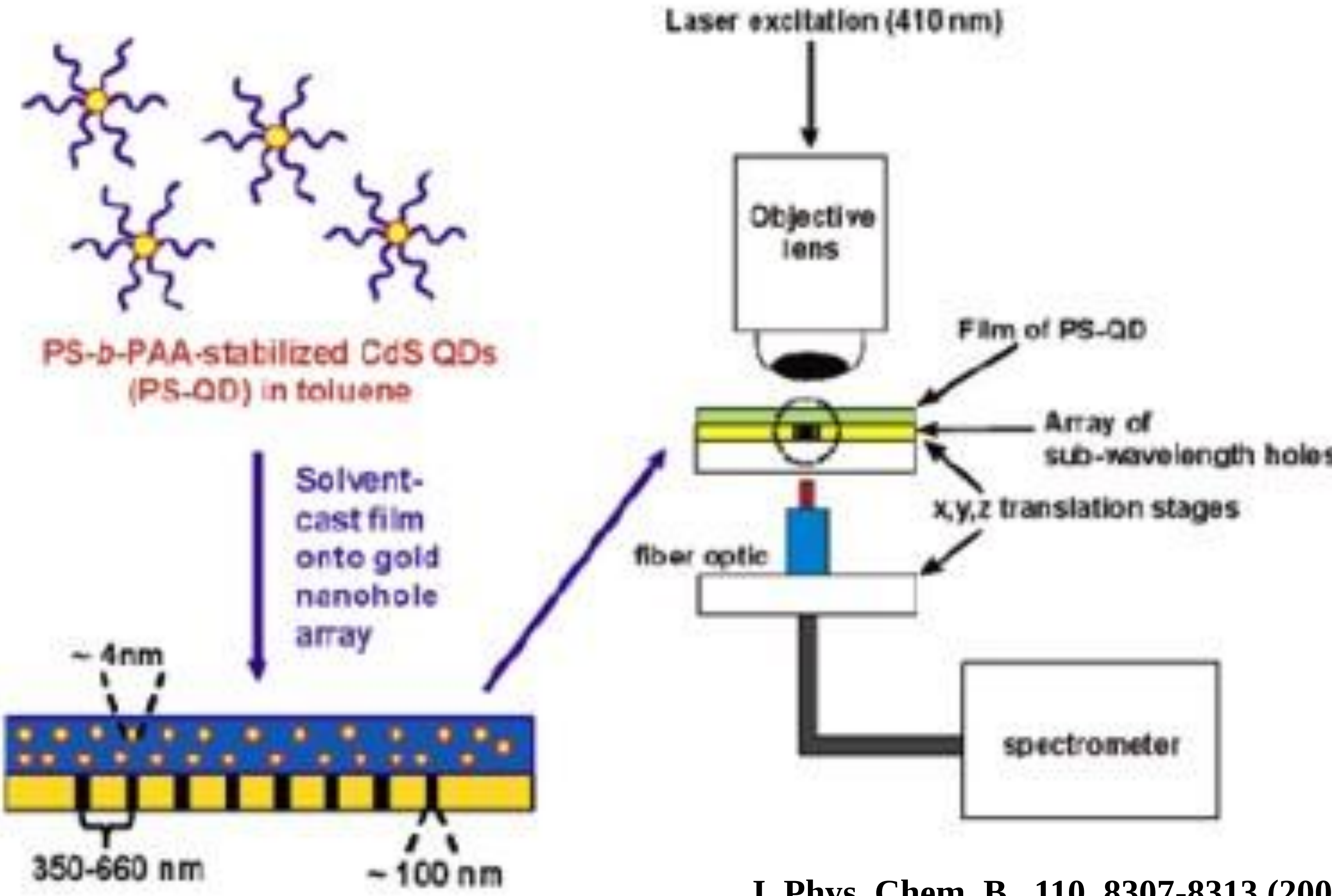

J. Phys. Chem. B., 110, 8307-8313 (2006).

Plasmonic Biosensors detects viruses

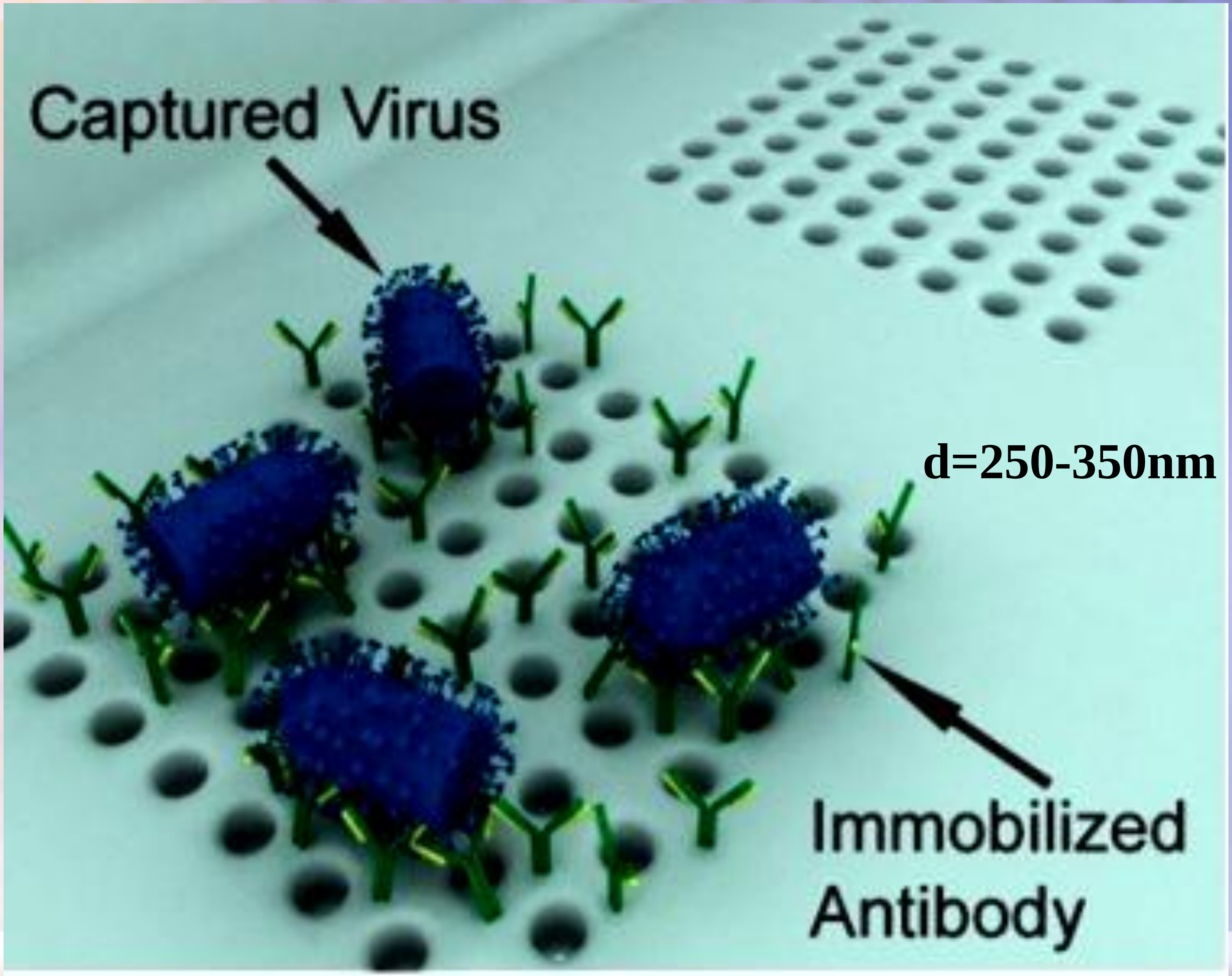

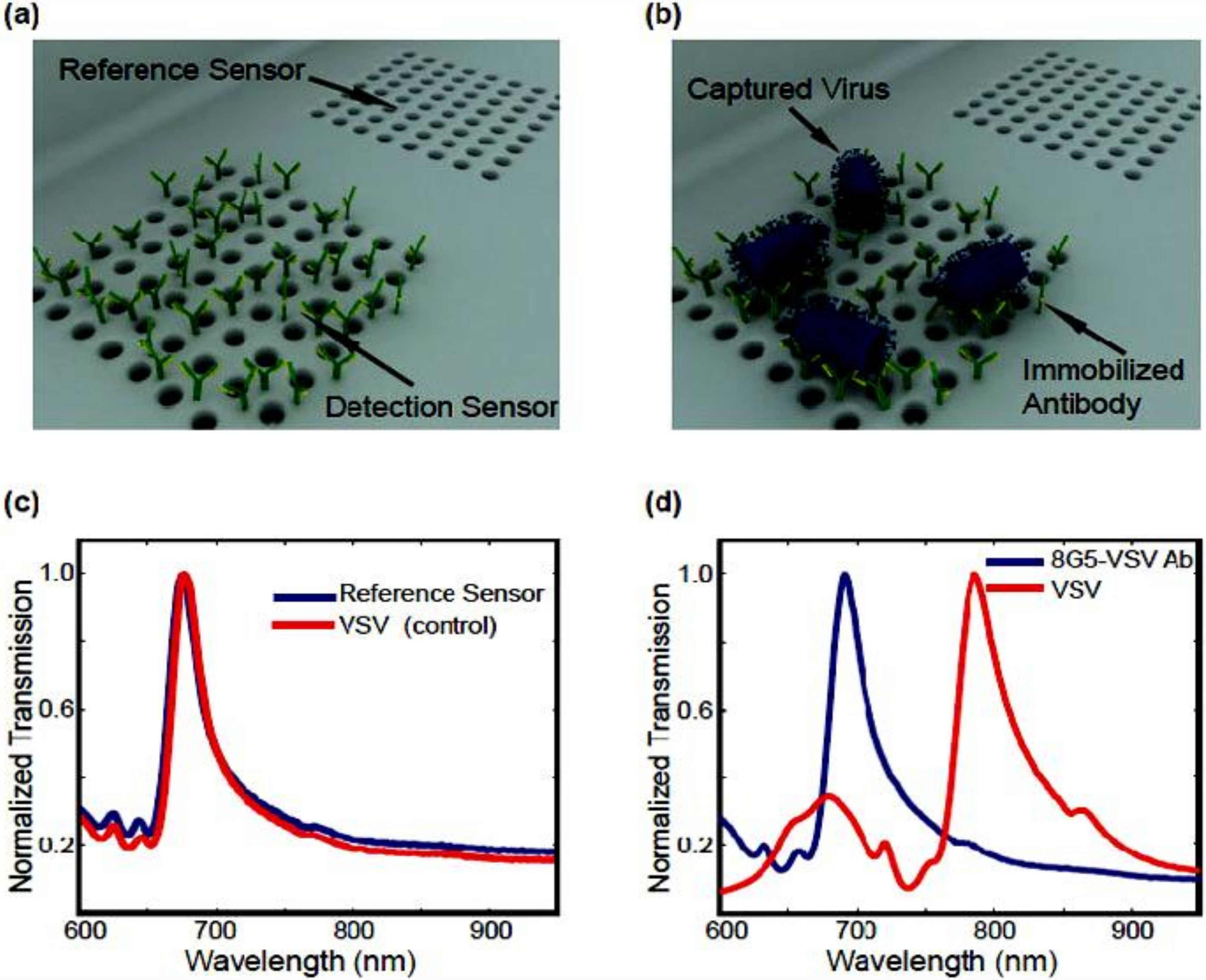
(a)
Reference Sensor
Detection Sensor
(b)
Captured Virus
Immobilized Antibody
(c)
Reference Sensor
VSV (control)
Normalized Transmission
1.0
0.6
0.2
600
700
800
900
Wavelength (nm)
(d)
8G5-VSV Ab
VSV
Normalized Transmission
1.0
0.6
0.2
600
700
800
900
Wavelength (nm)

IMMUNOASSAY

On-chip integration and application of nanoholes array

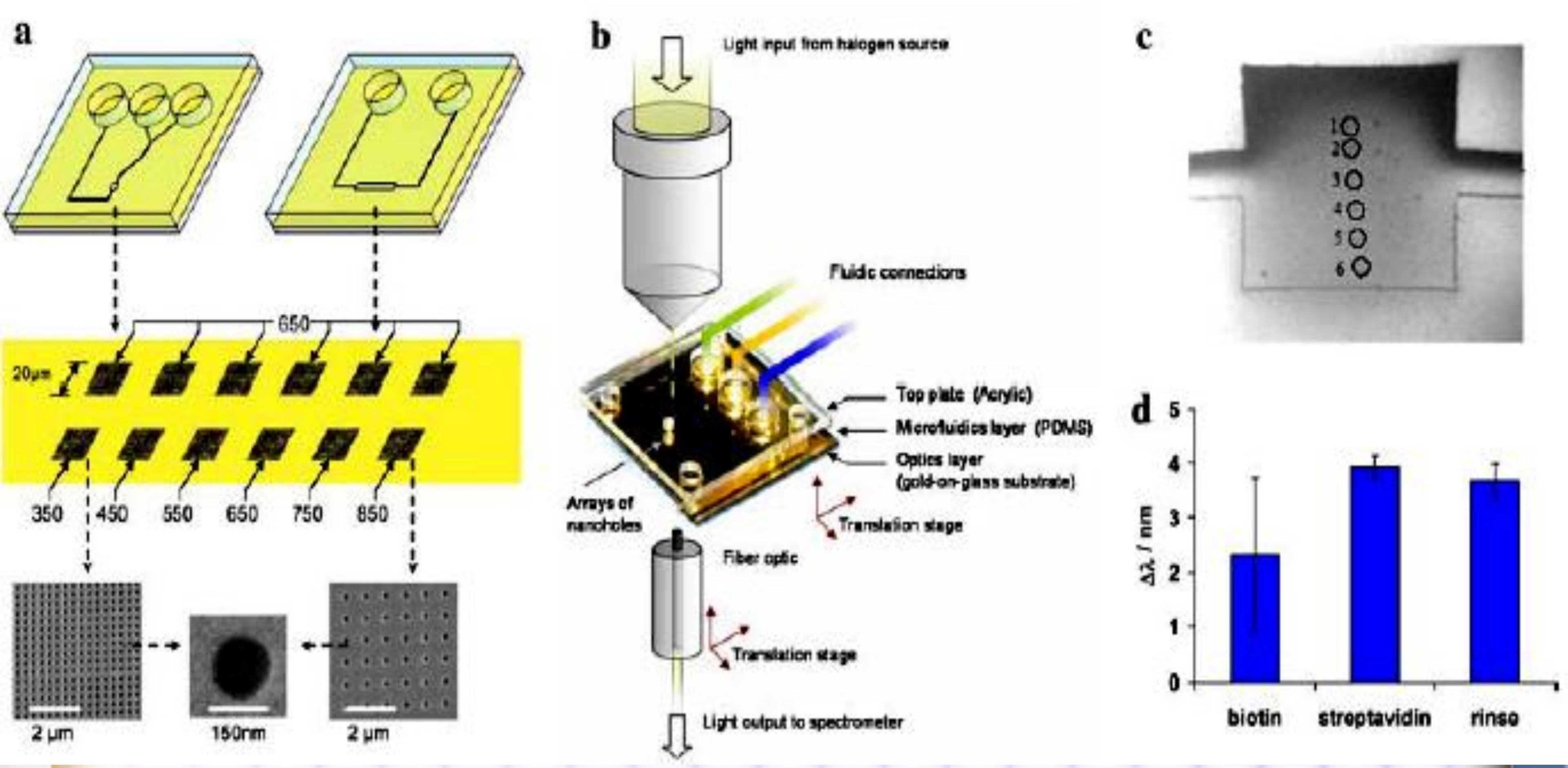

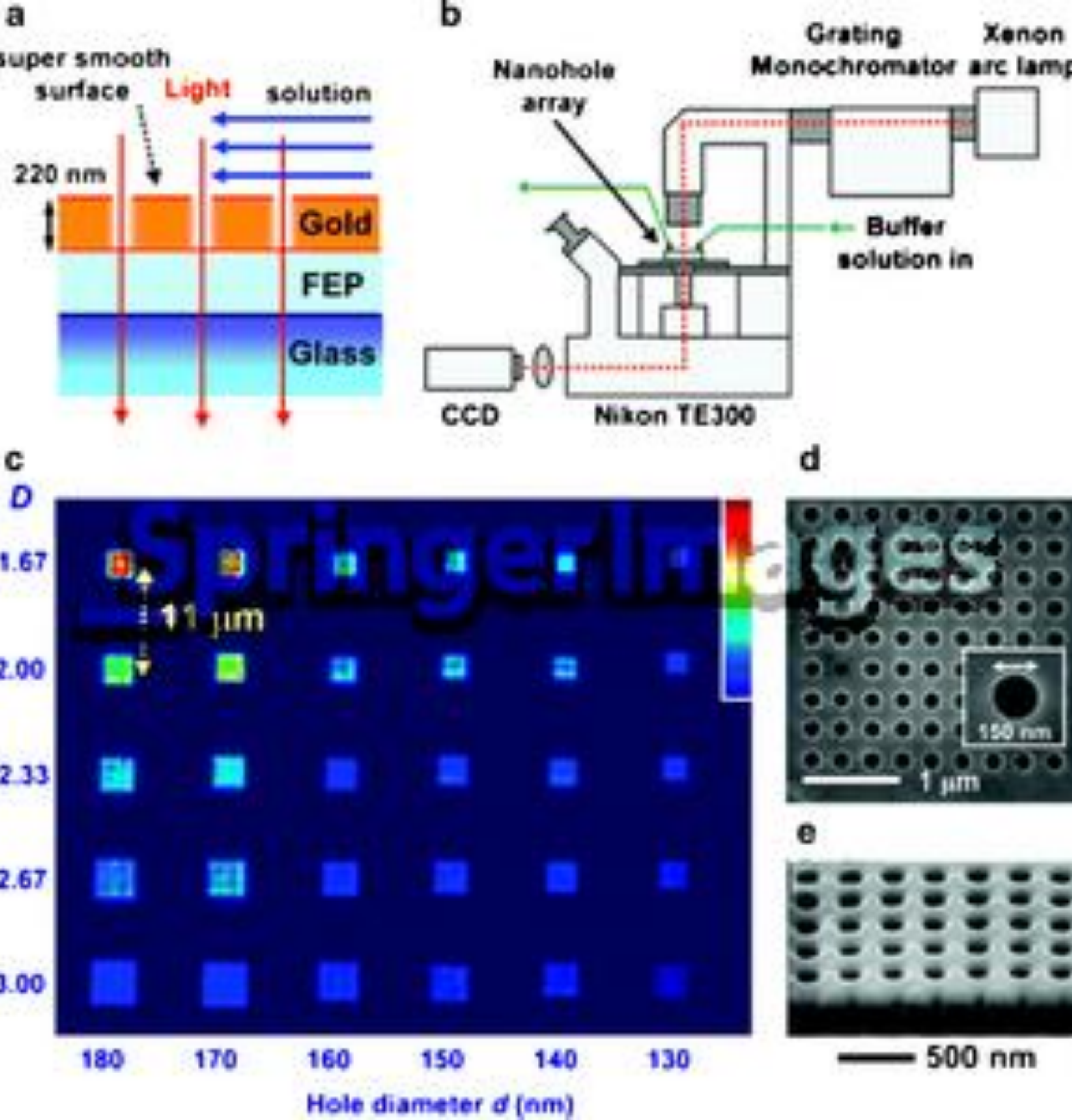

a Sample introduction onto a nanohole array biosensor.

b Nanohole array instrumental setup.

c CCD image of 30 sets of nanohole arrays **having different geometries**.

d, *e* SEM showing a top and a side view of a 9×9 nanohole array.

3D nanohole arrays for future plasmonic devices

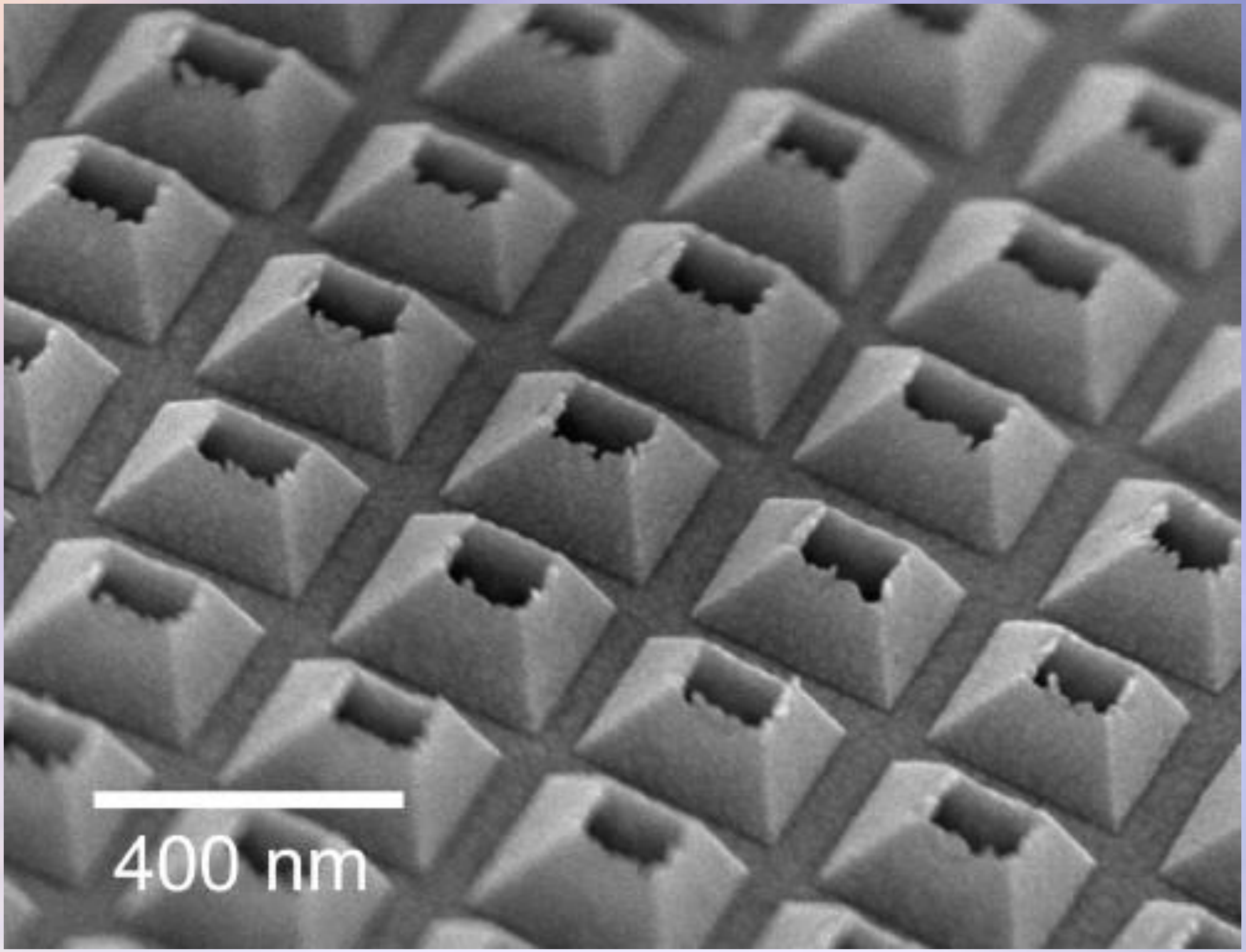

LSPs dominate the EOT more than SPPs on the same substrate.
Optical transmission from 3D hole arrays is an order of magnitude higher than that from 2D planar hole arrays.

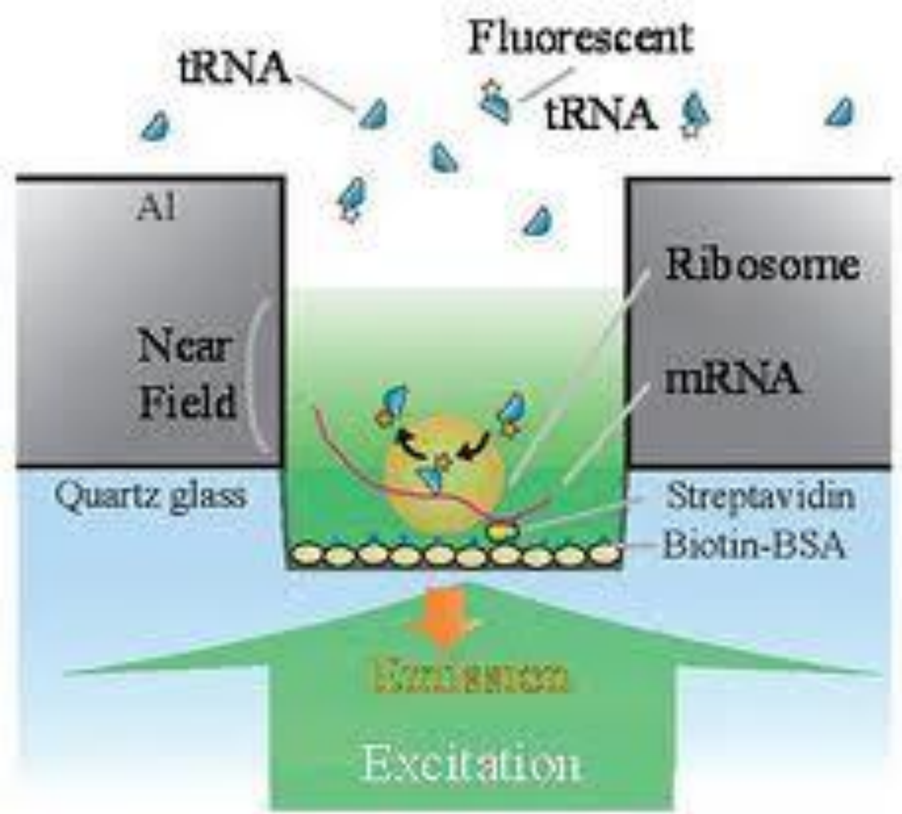
tRNA
Fluorescent
tRNA
Al
Ribosome
Near
Field
mRNA
Quartz glass
Streptavidin
Biotin-BSA
Excitation

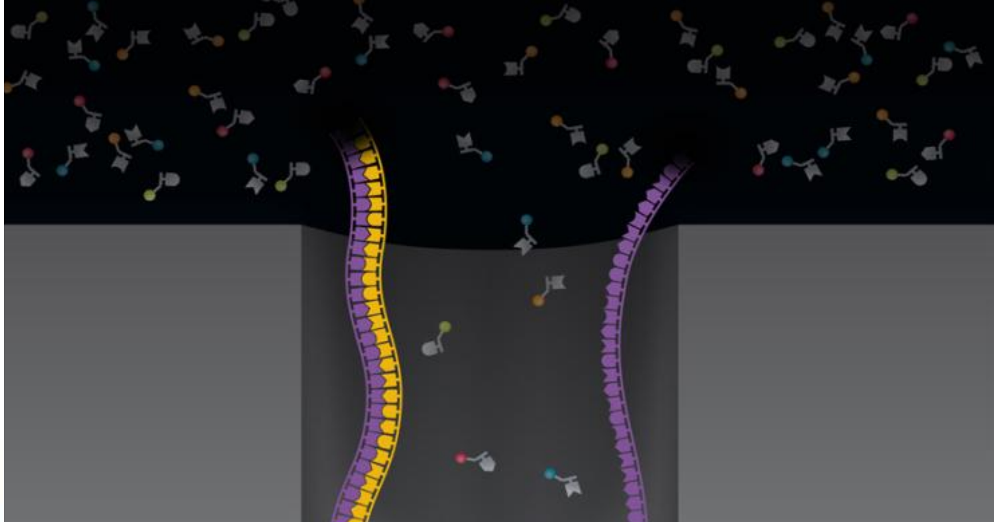

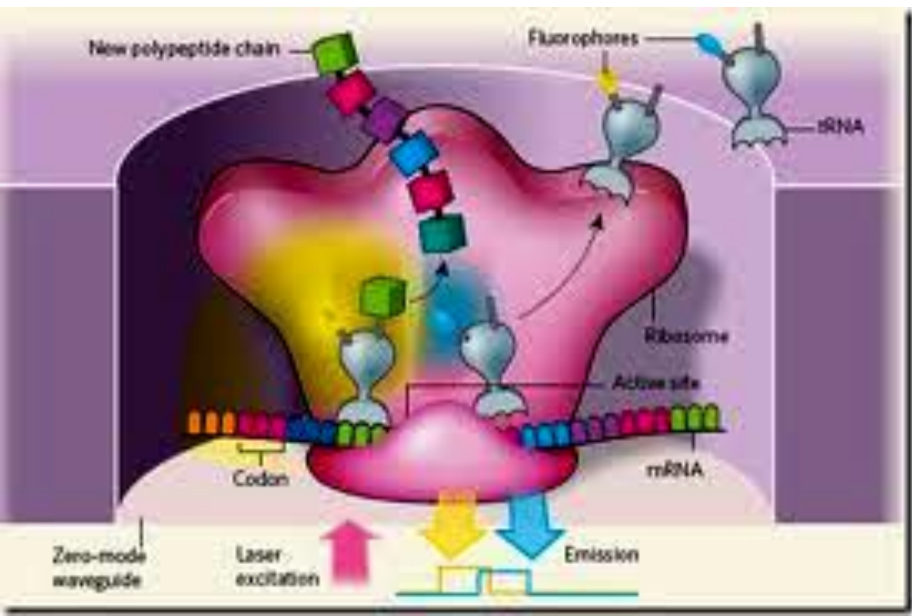
New polypeptide chain
Fluorophores
tRNA
Ribosome
Active site
Codon
mRNA
Zero-mode waveguide
Laser excitation
Emission

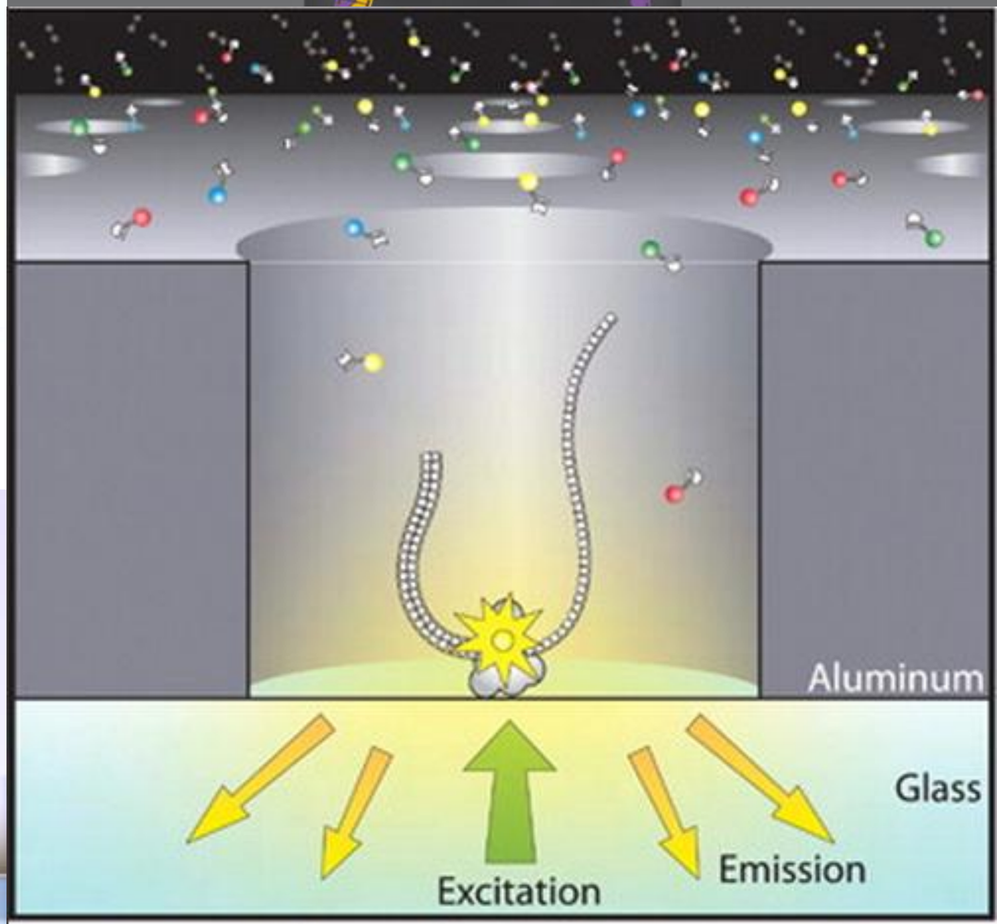
Aluminum
Glass
Emission
Excitation

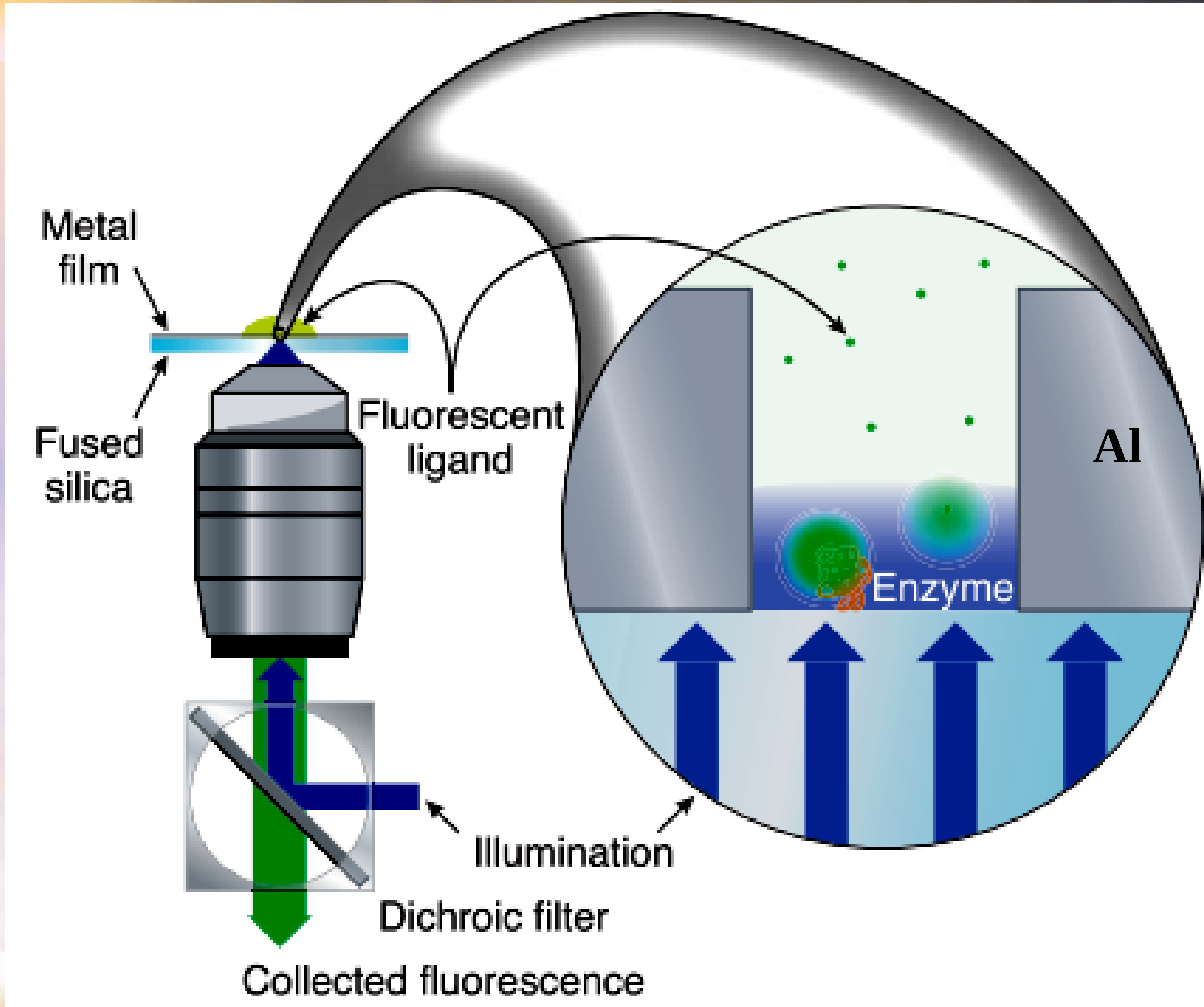
Metal film
Fused silica
Fluorescent ligand
Al
Enzyme
Illumination
Dichroic filter
Collected fluorescence

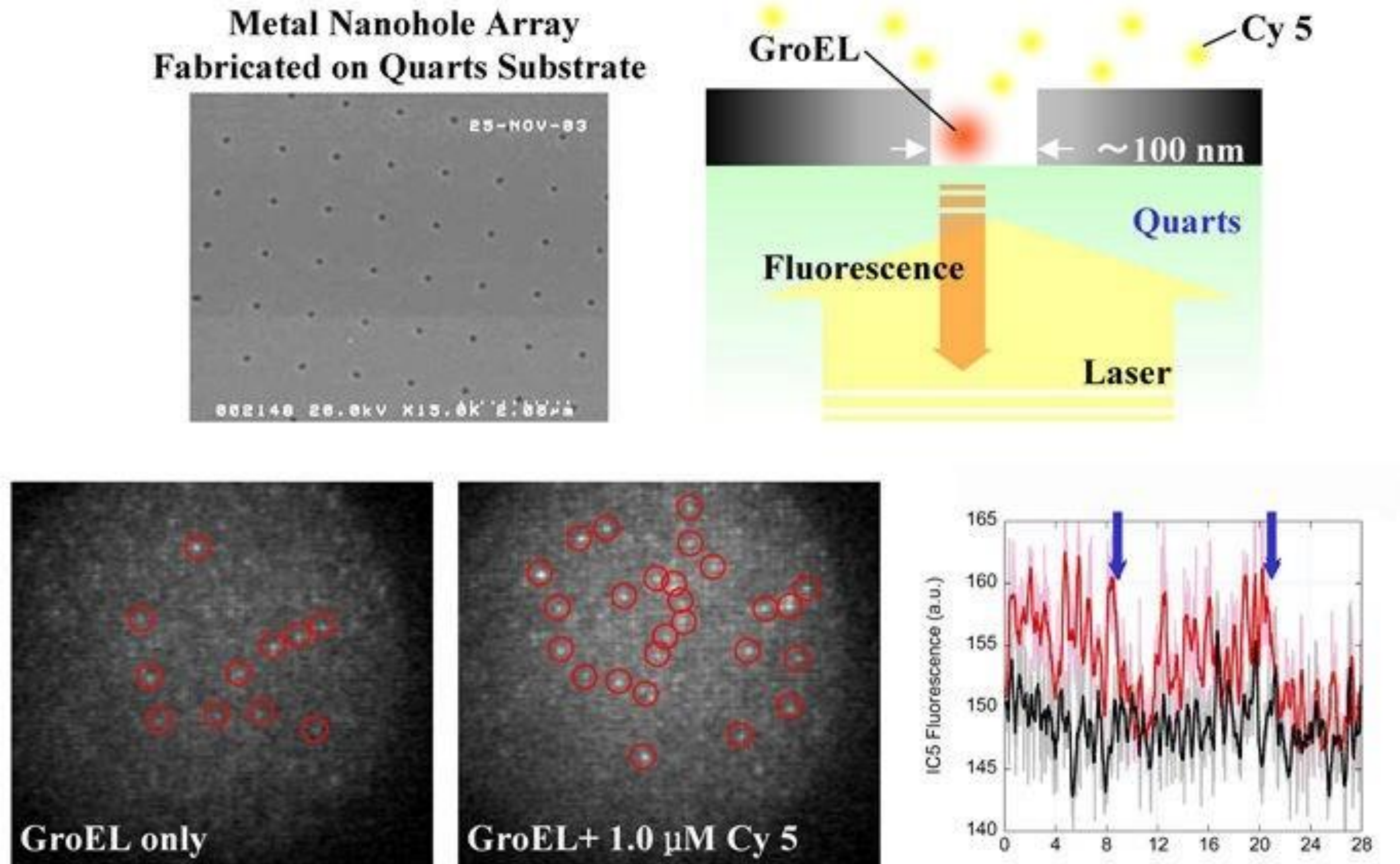

Fluorescence images of single GroEL enzymes labeled with IC-5 immobilized in the metal nanohole array on a quartz glass substrate. The quantized **photo-bleaching** proves the single molecule detection in each nanohole. The fluorescent dye Cy-5, which is diffused in water so that it mimics a protein in order to interact with GroEL, does not produce background noises because the laser light is guided only to the immobilized GroEL via the nanohole wave-guides.

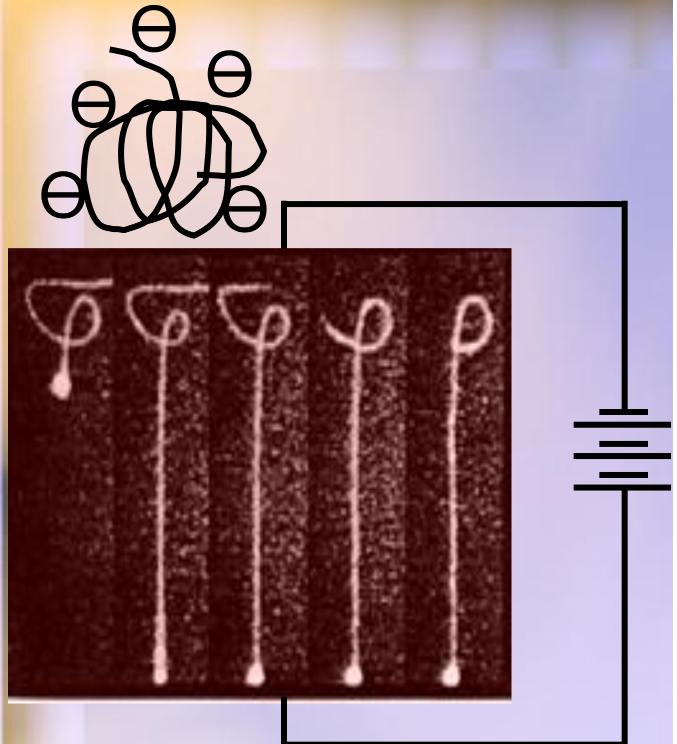

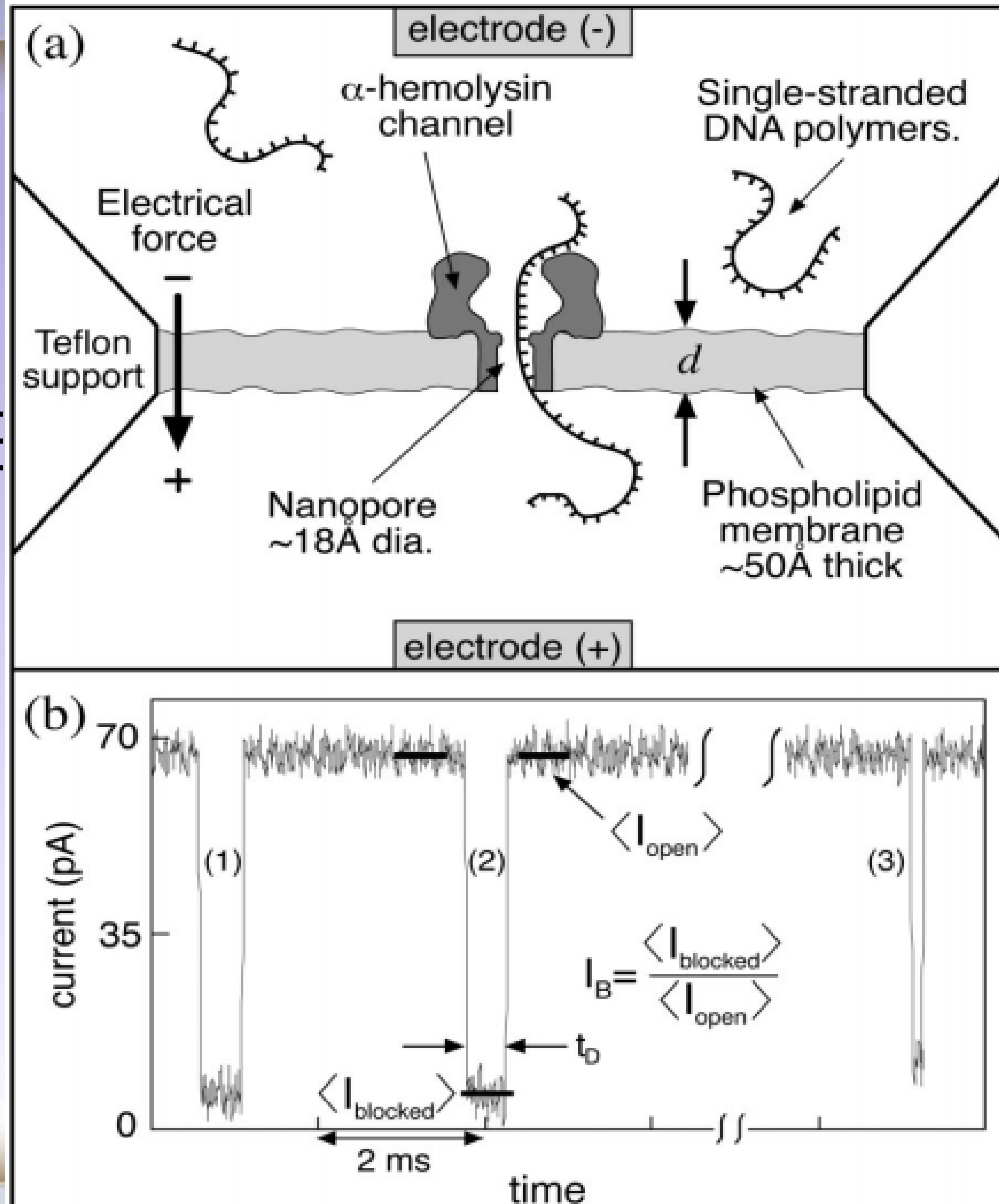

PRL, 86, 3435-3438 (2001)

双螺旋DNA结构图

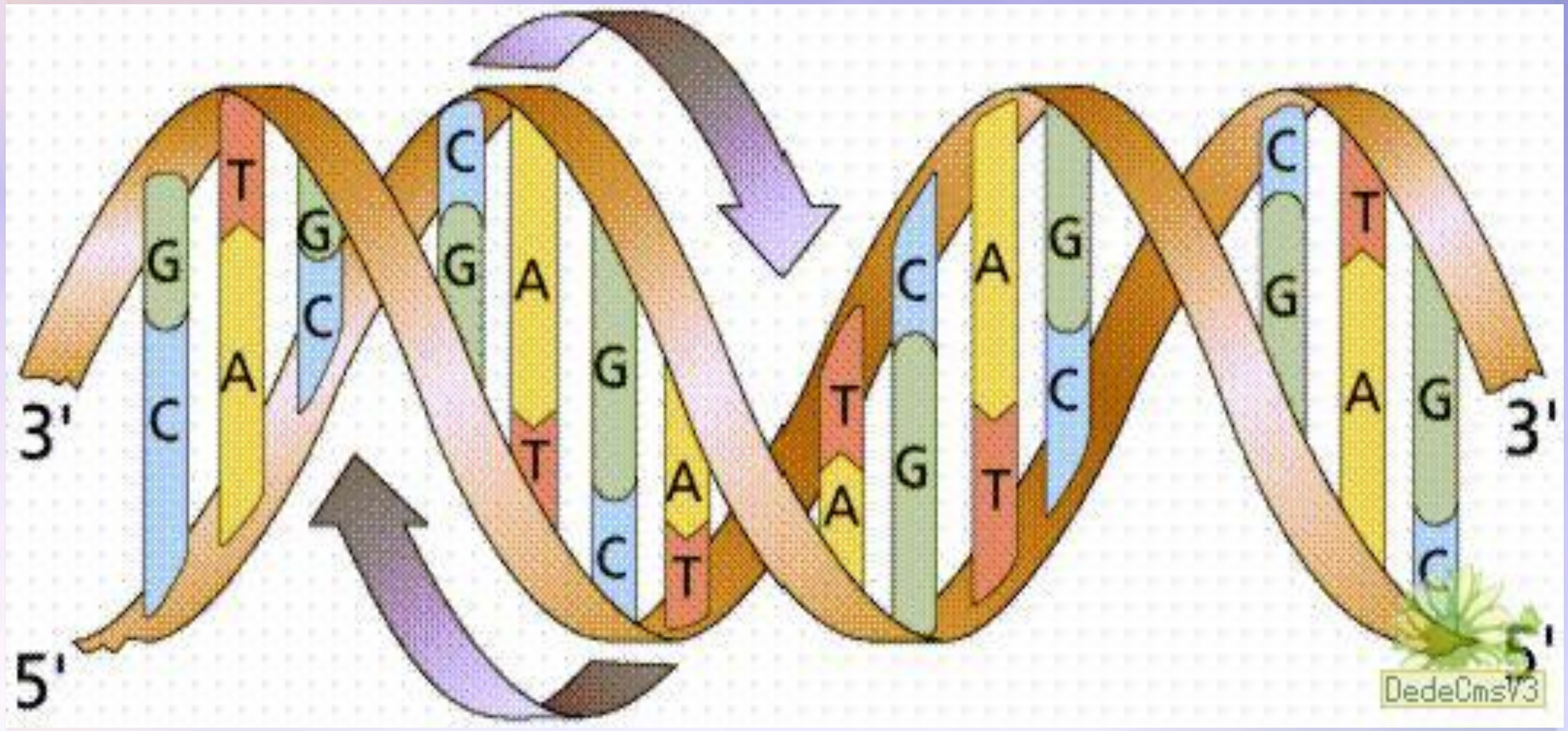

A hybrid plasmonic-photonic nanodevice for label-free detection of a few molecules

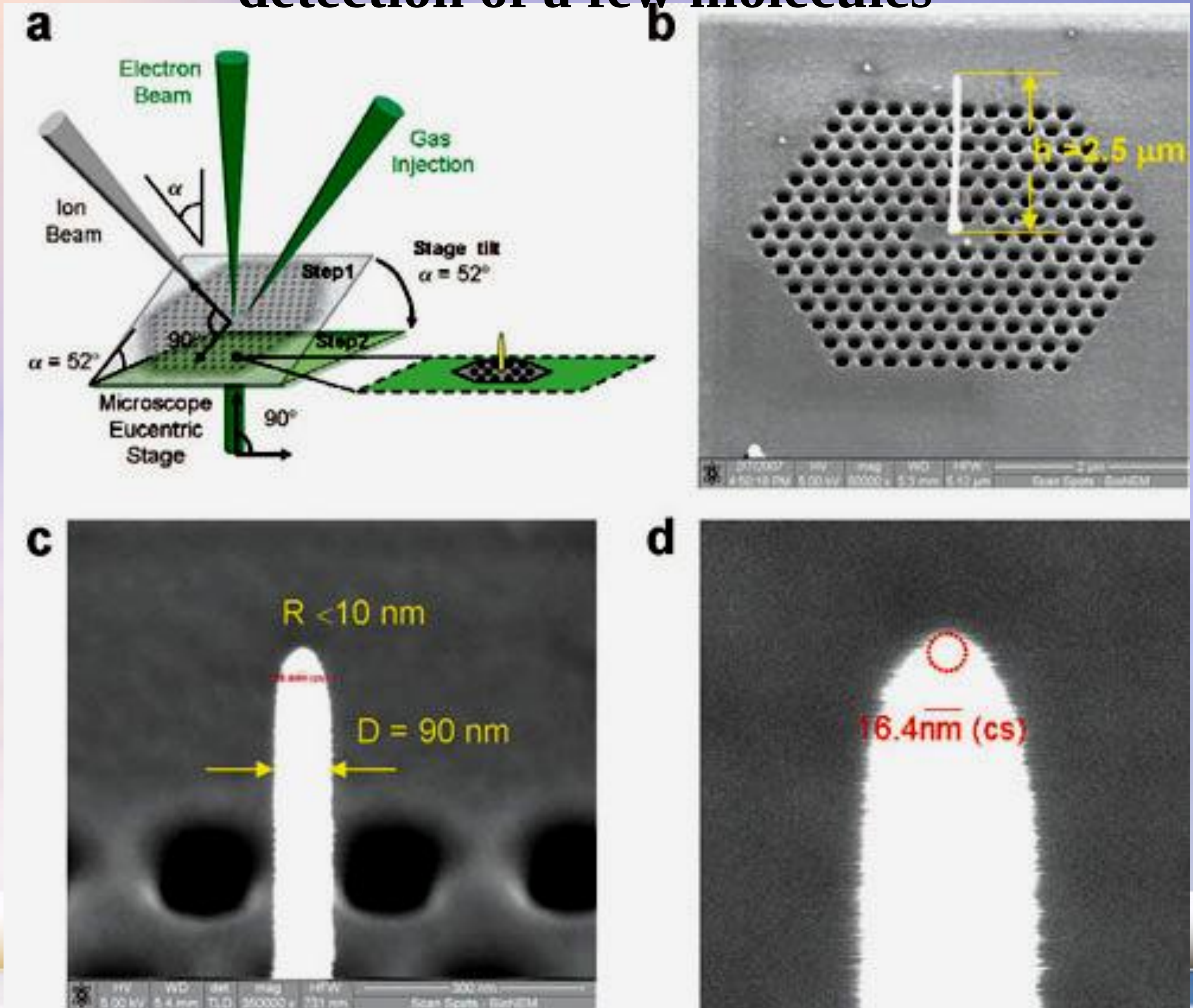

电子科技大学

University of Electronic Science and Technology of China

THE END

物理电子学院

School of Physical Electronics